

Tachyon field collapse - I: Inverse triad corrections

Y. Tavakoli,^{1,*} P. Vargas Moniz,^{1,2,†} J. Marto,^{1,‡} and A. H. Ziaie^{3,§}

¹*Departamento de Física, Universidade da Beira Interior, 6200 Covilhã, Portugal*

²*CENTRA, IST, Av. Rovisco Pais, 1, Lisboa, Portugal*

³*Department of Physics, Islamic Azad University, Kahnooj Branch, Kerman, Iran*

(Dated: June 2, 2019)

A marginal Lemaitre-Tolman-Bondi setting with a tachyon field, ϕ , is considered herein, as a model for gravitational collapse. The tachyon potential is assumed to be of inverse square form, i.e., $V(\phi) \sim \phi^{-2}$. In the classical regime, employing a dynamical system analysis complemented by a numerical study, we find asymptotic solutions approaching an homogeneous dust-like collapse; The corresponding final state points to a black hole formation. We then investigate whether modifications imported from loop quantum gravity can modify the outcome of the collapsing scenario. Restricting ourselves to inverse triad corrections, we obtain, within a semiclassical regime, several classes of analytical as well as numerical solutions. A qualitative analysis provides an attractor solution for the collapsing system. Our results indicate that this specific loop quantum effect induces an outward energy flux with neither a black hole nor a naked singularity emerging. The conclusions in this paper are supported by an analysis involving scaling solutions and a Hamilton-Jacobi description, where a broader potential of the form ϕ^{-P} is employed.

PACS numbers: 04.20.Dw, 98.80.Cq, 04.60.Pp

Keywords: Gravitational collapse, tachyon field, loop quantum gravity

I. INTRODUCTION

About forty years ago or so, S. Hawking and R. Penrose proved a series of powerful theorems that constitute the fundamental pillars to discuss the final fate of gravitational collapse [1–4], which may correspond either to a black hole or a naked singularity. It then became clear that general relativity was an incomplete theory and a quantum theory of gravity was mandatory [5], such that it would be singularity free¹.

Different matter contents have been explored regarding the process of gravitational collapse and specifically, the contribution of scalar fields has been a fructuous direction of research. Numerical [9] and analytical [10] classical solutions were retrieved, with particular interest given to the so-called cosmic censorship conjecture articulated by Penrose [11]. Initially, the scalar field was massless and free; Then, more elaborated settings followed introducing a wider class of potentials [12, 13]. Scalar fields therefore offer a rich framework to investigate the final state of gravitational collapse. Namely, which outcomes can be predicted? And if quantum effects are present, would they induce a different scenario? Would black holes form but then evaporate or would instead naked singularities form and dominate? References [4, 13], [14–24] constitute

a possible reading set, covering existing case studies.

In the above context, the objective of this paper is to investigate how specific loop quantum effects² can influence the collapse of a scalar field. More concretely, our framework is characterized by employing a tachyon field as the matter content and is motivated as follows:

- On the one hand, loop quantum effects within a semiclassical discussion may enlarge the range of dynamical possibilities. For example, in cosmological inflation [6], anti-friction effects occur when dealing with a standard scalar field initially rolling down a ϕ^2 potential, inducing the pulling of the field upwards. When employed within gravitational collapse, those loop effects could determine an outcome different from the classical setting; See [23, 24]: When dealing with fluid matter, the singularity prevails [23], while a *standard* scalar field as source points to a different final state [24].
- On the other hand, non-canonical scalar field theories have been attracting considerable attention (namely, ‘k-essence’ [25] and ‘k-inflation’ [26] scenarios). In particular, the action for the tachyon field³ has a *non-standard* kinetic term. The tachyon can act as a source for several effects, whose dynamical consequences are different from those of a standard scalar field [30–36]. In particular, it can also induce (anti-)friction effects.

*Electronic address: tavakoli@ubi.pt

†Electronic address: pmoniz@ubi.pt

‡Electronic address: jmarto@ubi.pt

§Electronic address: ah.ziaie@gmail.com

¹ In cosmological scenarios, for specific cases, singularities may be avoided, owing to, e.g., (i) bouncing effects imported from loop quantum gravity (LQG) [6] or (ii) a non-singular wave function for the universe (cf. [7, 8]).

² I.e., induced from LQG.

³ The (rolling) tachyon is an (unstable) field which emerges in (the low energy sector of) type II open string theory (through its role in the Dirac-Born-Infeld action, which is used to describe the (non-BPS) D-brane action [27–29]).

We organized this paper in the following manner. We start by presenting in section II a brief summary on Lemaitre-Tolman-Bondi (LTB) gravitational collapse within a perfect fluid setting. This is followed in section III by a discussion of LTB gravitational collapse with a tachyon field: In subsection III.A we use a phase space analysis to investigate the dynamics; Section III.B provides a complementary numerical study. In section IV we address whether quantum modifications can change the outcome retrieved in the previous section, reporting on a semiclassical study based on loop quantum corrections (of the inverse triad type): Subsection IV.A conveys a dynamical system analysis; A subsequent discussion employing a numerical investigation is presented in subsection IV.B (where we contrast the dynamical possibilities with those conveyed in III.B). In section V, we present our conclusions and a discussion of our results. Finally, we provide in appendix A a class of semiclassical collapsing trajectories, constituting scaling solutions, which is followed by an analysis, in appendix B, of loop quantum modifications on the tachyon field collapse from an Hamilton-Jacobi perspective.

II. A BRIEFING ON LTB GRAVITATIONAL COLLAPSE

In general relativity there is an exact solution which describes a spherically symmetric collapse in comoving coordinates: the LTB solution [37]. Considering a *marginally bound case* [4], where the interior spacetime is dynamical, we parameterize its line element as follows [13],

$$ds^2 = -dt^2 + a^2(t)[dr^2 + r^2 d\Omega^2], \quad (1)$$

where t is the proper time for a falling observer whose geodesic trajectories are labeled by the comoving radial coordinate r and $d\Omega^2$ being the standard line element on the unit two-sphere⁴; We have set the units $8\pi G = c = 1$. Then, the dynamical evolution of the system is determined by solving Einstein's field equations, which for the LTB solution with marginal bound case (1) can be presented [4] as,

$$\rho = \frac{F_{,r}}{R^2 R_{,r}}, \quad p = \frac{-\dot{F}}{R^2 \dot{R}}, \quad (2)$$

$$\dot{R}^2 = \frac{F}{R}. \quad (3)$$

The quantity $F(R)$ is the mass function of the collapsing matter, with $R(t, r) = ra(t)$ being the the area radius of

the collapsing shell, which is a function of the comoving coordinates t and r . The notation “,” and “.” denote a derivative with respect to r and the proper time, respectively. Since we are interested in a continuous collapsing scenario, the time derivative of the scale factor should be negative ($\dot{a} < 0$), implying that the area radius of the collapsing shell, for a constant value of r , decreases monotonically.

In order to illustrate a LTB gravitational collapse process, let us employ a particular class of solutions. We assume that the behavior of the matter density, for $a \ll 1$, is given by the following *ansatz* (cf. ref. [13, 15]),

$$\rho(t) \approx \frac{c}{a^n}, \quad (4)$$

where c and n are positive constants⁵. In this context, the matter content is described phenomenologically by a perfect (barotropic) fluid. To discuss the final state, it is important to study the geometry of a trapped surface in this spacetime. Let us be more precise and introduce key concepts that will assist us throughout this paper. A spherically symmetric spacetime containing a trapped region is characterized by the corresponding boundary (trapped) surface, extracted from the equation $F = R$. In the region where the mass function satisfies the relation $F > R$, it describes a trapped region and the regions i.e., $F < R$, are not trapped. In other words, if in a region of spacetime there exists a congruence of future directed non-spacelike trajectories emerging from a past singularity reaching distant observers, then a naked singularity may occur. But if no such families exist, trapped surfaces will form early enough and then regions will be hidden behind the event horizon, leading to the formation of a black hole [3, 4]. Furthermore, it is also useful [15] to define the deviation of a congruence of null geodesics, Θ , in the chosen spacetime [39]. A trapped surface⁶ is then defined as a compact two-dimensional (smooth) space-like surface S having the property that the parameter Θ of outgoing future-directed null geodesics, which are orthogonal to S , is everywhere negative on S [40]. For the marginal case of collapse described in (1)-(3), this parameter is given by

$$\Theta = \frac{2}{r} \left(1 - \sqrt{\frac{F}{R}} \right) \xi^r, \quad (6)$$

where ξ^r are defined as 4-vectors tangent to the geodesics

⁵ Using the energy density (4) and pressure (8), the weak energy condition can be written as follows

$$\rho + p = \frac{nc}{3a^n} > 0. \quad (5)$$

The weak energy condition is satisfied throughout the classical collapse process.

⁶ Generally speaking, at the initial epoch, there should not be any trapped surfaces due to the regularity conditions [4].

⁴ The interior spacetime of a collapsing configuration can be matched to a generalized Vaidya exterior geometry at a suitable boundary [38].

in spacetime. Integration of equation (2) gives the following relation for the mass function as

$$F = \frac{1}{3}\rho(t)R^3. \quad (7)$$

From equation (4), we may easily find a relation between the energy density and pressure as

$$p = \frac{n-3}{3}\rho. \quad (8)$$

Then, we can write equation (7) as $F/R = \frac{1}{3}\rho(t)r^2a^2$. Using this relation together with equations (3) and (4), bearing in mind the continuous collapse process ($\dot{a} < 0$), we get the time dependence of the scale factor as

$$a(t) = \left(a_0^{\frac{n}{2}} + \frac{n}{2}\sqrt{\frac{c}{3}}(t_0 - t) \right)^{\frac{2}{n}}, \quad (9)$$

where t_0 is the time at which the energy density begins increasing as a^{-n} and a_0 is the scale factor corresponding to t_0 . Assuming that the collapse process initiates at $t_0 = 0$, the time at which the scale factor vanishes corresponds to $\tilde{t}_s = \frac{2}{n}\sqrt{\frac{3}{c}}a_0^{n/2}$, implying that the collapse ends in a finite proper time. Also as a consequence, we can retrieve

$$\frac{F}{R} = \frac{c}{3}r^2a^{2-n}. \quad (10)$$

It is therefore possible to identify the following outcomes:

- For $0 < n < 2$, the quantity F/R is always less than unity throughout the collapse and if no trapped surfaces exist initially due to regularity condition, then no trapped surfaces would form until the epoch $a(t_s) = 0$. More precisely, Θ continues to be positive up to the singular epoch, with families of outgoing radial null geodesics emerging from a naked singularity. Consistently, the positiveness of Θ means that the covariant divergence of the vector tangent to radial null geodesics is always positive.
- For $n \geq 2$, trapped surfaces will form as the collapse evolves. Expressing in terms of Θ , as the collapse scenario progresses, we have that the ratio $F/R \rightarrow \infty$, and hence $\Theta \rightarrow -\infty$, which means that a singularity will be covered and no radial geodesics can emerge from it; Hence, a black hole forms [39].

III. CLASSICAL TACHYON FIELD COLLAPSE

We will henceforth consider a scalar field as the matter involved in the physical process of gravitational collapse. However, instead of a standard case⁷, we will employ

herein a homogeneous tachyon, $\phi(t)$. The main ingredient is the *non-standard* kinetic term for the tachyon scalar field.

To investigate the gravitational collapse of a tachyon field, we make use of the line element (1), employing A. Sen's effective action, whose Lagrangian can be written as [27, 28]

$$L = -a^3V(\phi)\sqrt{1-\dot{\phi}^2}. \quad (11)$$

The corresponding energy density and pressure are given by

$$\rho(\phi) = \frac{V(\phi)}{\sqrt{1-\dot{\phi}^2}}, \quad (12)$$

$$p(\phi) = -V(\phi)\sqrt{1-\dot{\phi}^2}, \quad (13)$$

i.e., satisfying

$$p(\phi) = (\dot{\phi}^2 - 1)\rho(\phi), \quad (14)$$

where $V(\phi)$ is the tachyon potential. Using the equation for the energy conservation, $\dot{\rho} + 3H(\rho + p) = 0$, we get the equation of motion for the tachyon field ϕ as

$$\ddot{\phi} = -(1-\dot{\phi}^2) \left[3H\dot{\phi} + \frac{V_{,\phi}}{V} \right], \quad (15)$$

where “ $\dot{\phi}$ ” denotes the derivative with respect to the tachyon field and $H = \dot{a}/a$ is the Hubble rate.

A definitive form for the the tachyon potential $V(\phi)$ has not yet been established [30–34], but there are few proposals satisfying the (qualitative) requirements indicated by open string theory. Being more concrete, $V(\phi)$ should have a maximum at $\phi \sim 0$ and it should go to zero at infinite values of the tachyon field⁸. It has been argued [27–30] that $V(\phi)$ would have an exponential behavior, $V \sim e^{-\phi}$, or even a $\cosh^{-1} \phi$ form. An alternative has been to use an inverse power law, i.e.,

$$V \sim \phi^{-\mathcal{P}}, \quad (16)$$

\mathcal{P} being a positive constant (allowing for scaling solutions), from which the exponential potential can be suitably built [30–34]. Simple exact analytical solutions were found in [30]; Nevertheless, it can be argued that with this potential there is a divergence at $\phi \sim 0$, although it can be mentioned that it has the asymptotic behavior for a required tachyon potential. A thorough discussion on other potentials and contexts can be found in [33] and [36]. Throughout the main text of this paper we will focus only on an inverse power law potential

⁷ A standard scalar field was considered in [13, 24].

⁸ Such that in this asymptotic vacuum there are no D-branes and hence no open strings.

for the tachyon, more precisely with $\mathcal{P} = 2$, adopting a purely phenomenological perspective, likewise recent papers [30–35].

Before proceeding, let us mention the following. If we impose the ansatz (4) into the equations (8), (12) and (13), then (cf. also ref. [32])

$$w = \frac{p(t)}{\rho(t)} = \dot{\phi}^2 - 1 = \frac{n-3}{3}, \quad (17)$$

i.e., w is a constant and $\dot{\phi}$ likewise; From (17), this then leads⁹ to the range $0 \leq n \leq 3$. The final state of the collapse can be a naked singularity (cf. previous section) if $-1 < w \leq -1/3$. By means of $\dot{\phi} \equiv \dot{a}\phi_{,a}$, where $\phi_{,a}$ is the derivative of the scalar field with respect to scale factor, this allow us to write $\phi(a) = \frac{2}{\sqrt{nc}}a^{\frac{n}{2}}$.

Substituting the expression $\phi(a)$ in equations (12) and (17), the potential V can, in more detail, be expressed as $V(\phi) = \frac{\tilde{c}_n}{\phi^2}$, where $\tilde{c}_n \equiv \frac{4}{n}\sqrt{1-\frac{n}{3}}$.

Notwithstanding those results, the fact is that they only represent a particular outcome for the collapse, constituting a specific class of solutions, constrained by the ansatz (4); Equations (15), (16), with $\mathcal{P} = 2$, admit other solutions. A broader discussion is mandatory and this is brought in the next subsection, by means of a dynamical system analysis (see ref. [31–35, 41]).

A. Tachyon field collapse and phase space analysis

Let us then study the collapse of a tachyon field from a dynamical system perspective [41], without any *a priori* behavior constrained into the tachyon (e.g., cf. (4) in section II). This will provide a wider discussion of the tachyon evolution, within a gravitational collapse.

We define a new time variable τ (instead of the proper time t in the comoving coordinate system $\{t, r, \theta, \varphi\}$) for our collapsing system, as [35]

$$\tau \equiv -\log\left(\frac{a}{a_0}\right)^3, \quad (18)$$

which is defined in the interval $0 < \tau < \infty$; The limit $\tau \rightarrow 0$ corresponds to the initial condition of the collapsing system ($a \rightarrow a_0$), and the limit $\tau \rightarrow \infty$ corresponds to $a \rightarrow 0$. For any time dependent function $f = f(t)$, we can write¹⁰

$$\frac{df}{d\tau} \equiv -\frac{\dot{f}}{3H}, \quad (19)$$

where a dot over a variable denotes its derivative with respect to time t . Besides (15), the field equations for

tachyon field collapse within the marginal case of LTB setting, also comprise

$$3H^2 = \frac{V(\phi)}{\sqrt{1-\dot{\phi}^2}}. \quad (20)$$

and

$$-2\dot{H} = \frac{V(\phi)\dot{\phi}^2}{\sqrt{1-\dot{\phi}^2}}. \quad (21)$$

We will use an inverse power-law potential, (16), with $\mathcal{P} = 2$. A plot of $V(\phi)$ is qualitatively presented in Fig. 1; We can consider it as two (mirror) branches, upon the symmetry $\phi \rightarrow -\phi$, treating the $\phi > 0$ and $\phi < 0$ separately.

Introducing the new set of dynamical variables [35]

$$x \equiv \dot{\phi}, \quad y \equiv \frac{V}{3H^2}, \quad (22)$$

the constraint equation (20) becomes

$$\frac{y}{\sqrt{1-x^2}} = 1. \quad (23)$$

The dynamical variables have the range¹¹ $0 \leq y \leq 1$, $-1 \leq x \leq 1$, and $x^2 + y^2 = 1$. This will mean having to deal with an effective one-dimensional phase space (cf. [35, 42, 43]). Equations (20) and (21), together with (15) allow the corresponding autonomous system to be written as

$$\frac{dx}{d\tau} = f_1(x, y) \equiv \left(x + \frac{\lambda}{\sqrt{3}}\sqrt{y}\right)(1-x^2), \quad (24)$$

$$\frac{dy}{d\tau} = f_2(x, y) \equiv xy \left(\frac{\lambda}{\sqrt{3}}\sqrt{y} + x\right), \quad (25)$$

where

$$\lambda \equiv -V_{,\phi}/V^{3/2}, \quad (26)$$

which, for the inverse square potential of the form $V(\phi) = V_0\phi^{-2}$, determines that $\lambda = \pm\frac{2}{\sqrt{V_0}}$; Note that $\lambda > 0$ for the $\phi > 0$ branch and $\lambda < 0$ for the $\phi < 0$ branch. Using the condition $(f_1, f_2)|_{(x_c, y_c)} = 0$, we can obtain the critical points (x_c, y_c) of the autonomous system. We have the following points in the $\phi > 0$ branch¹²: (a) at

⁹ Note that the time derivative of the tachyon field is restricted to the interval $-1 \leq \dot{\phi} \leq 1$.

¹⁰ We recall that throughout this paper $H < 0$, i.e., $\dot{a} < 0$ is assumed.

¹¹ Note that $V(\phi) > 0$.

¹² The autonomous system presented herein is generic in terms of λ . That is, for the $\phi < 0$ branch, we would find $[a]$ at $(1, 0)$, $[b]$ at $(-1, 0)$ and $[c]$ at $(-\lambda\sqrt{y_0/3}, y_0)$, setting $\lambda = -\frac{2}{\sqrt{V_0}}$. Moreover, $y_0 = -\lambda^2/6 + \sqrt{(\lambda^2/6)^2 + 1} > 0$ and $-\lambda\sqrt{y_0/3} > 0$; The fixed point $[c]$ is in the first quadrant of the phase plane.

(1,0), (b) at $(-1,0)$ and (c) at $(-\lambda\sqrt{y_0/3}, y_0)$, where $y_0 = -\lambda^2/6 + \sqrt{(\lambda^2/6)^2 + 1} > 0$; Cf. figures 1, 3 and 4.

Regarding their stability analysis, for small (linear) perturbations $(\delta x, \delta y)$, i.e.,

$$x = x_c + \delta x, \quad y = y_c + \delta y, \quad (27)$$

using the autonomous system (24)-(25) and neglecting higher order terms in perturbations, it leads to

$$\frac{d}{d\tau} \begin{pmatrix} \delta x \\ \delta y \end{pmatrix} = \mathcal{A} \begin{pmatrix} \delta x \\ \delta y \end{pmatrix}, \quad (28)$$

where the matrix \mathcal{A} is defined at each fixed point (x_c, y_c) as

$$\mathcal{A} = \begin{pmatrix} \frac{\partial f_1}{\partial x} & \frac{\partial f_1}{\partial y} \\ \frac{\partial f_2}{\partial x} & \frac{\partial f_2}{\partial y} \end{pmatrix} \Big|_{(x_c, y_c)}. \quad (29)$$

From the eigenvalues of \mathcal{A} , the stability can be determined by means of

$$\delta q_i(\tau) = \sum_j^k (q_0)_i^j \exp(\zeta_j \tau), \quad (30)$$

where $q_i = (q_1, q_2) \equiv (x, y)$ and ζ_j are the eigenvalues of the matrix \mathcal{A} ; The $(q_0)_i^j$ are constants of integration. In more detail (where Table I provides a more compact summary):

point	x	y	w_ϕ	Existence	Stability
(a) ([a])	1	0	0	for $\lambda > 0$ (for $\lambda < 0$)	Stable node (attractor)
(b) ([b])	-1	0	0	for $\lambda > 0$ (for $\lambda < 0$)	Stable node (attractor)
(c) ([c])	$-\lambda\sqrt{y_0/3}$	y_0	$-y_0^2$	for $\lambda > 0$ (for $\lambda < 0$)	Unstable (source)

TABLE I: Summary of critical points and their properties for the $\phi > 0$ and $\phi < 0$ branches (Cf. Fig. 1, 3 and 4).

- Point (a): The eigenvalues are $\zeta_1 = -2$ and $\zeta_2 = -1$. Since both are real and negative, the exponential terms $\delta x(t) \approx \exp(-2\tau) = (a/a_0)^6$ and $\delta y(t) \approx \exp(-\tau) = (a/a_0)^3$ decay as τ increases (i.e. a decreases) and tend to zero as $\tau \rightarrow \infty$ (i.e. $a \rightarrow 0$) (cf. eq. (30)). Therefore, a trajectory near this fixed point will converge towards it; This point is an asymptotically *stable* node (attractor), allowing to select to a class of solutions in which, from $\dot{\phi} \simeq 1$, the corresponding (asymptotic) time dependence of the tachyon field can be estimated as

$$\phi(t) \simeq t + \phi_0, \quad (31)$$

where ϕ_0 is the value at the initial configuration of the collapsing system. In particular, within the $\phi > 0$ branch, we can consider the case of the tachyon field starting to increase with time from its initial value (when $t = 0$ with $\phi(t = 0) = \phi_0 > 0$), proceeding downhill the potential. Complementary dynamical behaviors are conveyed in subsection III.B.

Moreover, the spacetime becomes singular at a finite amount of time, thus the tachyon field reaches

its maximum¹³ and remains finite (i.e. $\phi \rightarrow \phi_s$ as $t \rightarrow t_s < \phi_0$). Correspondingly, the potential contributes with its minimum (and nonzero value) at t_s . The dynamical variable $y = \frac{V}{3H^2}$ asymptotically vanishes as the Hubble rate H diverges. This shows that the energy density increases as $a \rightarrow 0$. Furthermore¹⁴ from (14), the effective pressure asymp-

¹³ The tachyon field (31) evolves until it reaches the singular state at $a = 0$. Let us consider the scale factor as a monotonically decreasing function of time. Then, the energy density (12) can be written as a function of a as

$$\rho \equiv 3 \left(\frac{\psi(a)}{a} \right)^2, \quad (32)$$

where $\psi \in C^\infty(0, a_0)$. From the constraint, $\rho = 3H^2$, eq. (20), we have $\psi(a) = -\dot{a}$. Moreover, the collapse implies that $\psi(a)$ should be positive. Using the properties of $\psi(a)$, it can be shown (cf. ref. [44]) that the spacetime becomes singular in a finite amount of comoving time t , if and only if $1/\psi(a)$ is integrable on $(0, a_0)$. This time is finite and is given by $t_s = \int_0^{a_0} da/\psi(a)$. The tachyon field, in this process, will not diverge and the tachyonic potential will reach $V_s \equiv V(\phi_s) > 0$.

¹⁴ On the other hand, for the $\phi < 0$ branch, as the collapsing system starts its evolution from an adequate initial condition, as time evolves, the tachyon field may increase, i.e., proceed to ever less negative values as $\phi \rightarrow 0^-$. In this case, which is associated to the point [a] (cf. Fig. 1) and is the asymptotic stage in the

totically vanishes. This suggests a dust-like behavior (cf. also subsection III.B; Figs. 5 and 6).

Let us be more concrete and in order to reach that purpose we rewrite equations (2) and (3), where $p \simeq 0$, as [4]

$$R^{3/2}(t, r) = r^{3/2} - \frac{3}{2}\sqrt{F}(t - t_i). \quad (33)$$

Using the freedom in scaling the comoving coordinate r , we have set here an initial condition at $t = t_i$, namely $R(t_i, r) = r$, at the starting epoch for this regime. Moreover, regularity conditions for initial data impose $F(t_i, 0) = 0$, that is, the mass function should vanish at the central singularity (i.e., $r = 0$). The collapsing time can be obtained by setting $R(t_s(r), r) = 0$ and is given by¹⁵ $t_s(r) = \frac{2r^{3/2}}{3\sqrt{F}} + t_i$. Substituting $t_s(r)$ in equation (33), we get the scale factor as

$$a(t) = \left(1 - \frac{3}{2}\sqrt{\frac{F}{r^3}}(t - t_i)\right)^{2/3}. \quad (34)$$

In this region, then $\dot{F} = 0$, that is, the mass function does not have any time dependence and is given by $F = F(r)$. Using equation (3), the mass function can be rewritten as $F(r) = r^3 a \dot{a}^2$. Regularity requires that $R(t, 0) = 0$ and $\frac{F}{r^3} < \infty$, as $r \rightarrow 0$. So, the term $a \dot{a}^2$ remains finite near the singularity, $\psi(a)$ takes the form $\psi(a) \propto -1/\sqrt{a}$ and thus, the energy density of collapse in equation (32) reads $\rho = \rho_\phi \propto 1/a^3$; This expression indicates, therefore that, ρ_ϕ diverges as $a \rightarrow 0$. In addition, the term $r^2 \dot{a}^2$ remains less than unity, $\frac{F}{R} < 1$, as $r \ll 1$ and thus, no trapped surfaces would form at the center (where $r = 0$): A naked singularity seems to occur. At this point, however, we must be careful: A dust-like behavior in a LTB gravitational collapse setting conveys a black-hole; Cf. [18].

Let us subsequently complement our discussion, studying the behavior of the apparent horizon for the homogeneous model herein: The boundary of the trapped region is the apparent horizon, which

determines the formation of a black hole. In a spherically symmetric spacetime, it is given by the curve¹⁶ $R(t_{\text{ah}}(r), r) = F(r)$. Using this relation in (33) we have

$$t_{\text{ah}}(r) = \frac{2r^{3/2}}{3\sqrt{F}} - \frac{2}{3}F(r), \quad (35)$$

which gives the time at which the apparent horizon forms. Equation (35) shows that shells with $r > 0$ become trapped before eventually reaching the central singularity (i.e. where $r = 0$) at time t_s . For the homogeneous model considered herein, it is seen that as the radius r decreases, the collapsing matter approaches the (central) singularity. Substituting the mass function $F(r) = F_0 r^3$ (where $F_0 = a \dot{a}^2$ is a constant near the singularity) in equation (35), it can be seen that trapped surfaces form in a finite time, given by

$$t_{\text{ah}}(r) = \frac{2}{3\sqrt{F_0}} - \frac{2}{3}F_0 r^3. \quad (36)$$

From the above equation, it is seen that $t_{\text{ah}}(r) < t_{\text{ah}}(0)$, implying that any neighborhood gets trapped before reaching the center. At this point, we will have $t_{\text{ah}}(0) = t_s(0)$ and the neighboring regions get trapped before a singularity forms. In other words, trapped surfaces will form early enough during the collapse, before any singularity is allowed to emerge later. This culminates in a spacetime event horizon, which fully covers a singularity and produces a black hole for the collapse final state. In subsection III.B we complement (and support) our discussion above by means of additional arguments, extracted from a thorough numerical analysis.

- Point (b): The eigenvalues are $\zeta_1 = -2$ and $\zeta_2 = -1$. This point also constitutes an asymptotically *stable* node (attractor). From (22), the time dependence of the tachyon field can be written as

$$\phi(t) \simeq -t + \phi_0 \quad (37)$$

for the $\phi > 0$ branch, with the tachyon field decreasing from its initial value at $t = 0$ (where $\phi_0 > 0$) and corresponding to motion uphill the potential. The potential will reach a maximum (but finite) value when the tachyon field reaches its minimum and nonzero value (i.e. $\phi \rightarrow \phi_s$ as $t \rightarrow t_s < \phi_0$). At this point, the Hubble rate increases faster than the potential and diverges. In

uphill potential approach, it so proceeds till the system reaches $a = 0$ at $t = t_s$, where the Hubble rate diverges. It should be noted that, in a continuous collapsing process, this implies that the time in which the collapse system reaches the singularity is always $t_s \leq \phi_0$.

¹⁵ In an inhomogeneous dust collapse, the (central) singularity occurs at $r = 0$, where the proper radius r vanishes. On the other hand, a curvature singularity can emerge at a nonzero physical radius $r > 0$, when $R(t_s(r), r) = 0$, being labeled as a shell-focussing singularity [45]. In a homogeneous model (like the Oppenheimer-Snyder model), these two types of singularities are coincident [46].

¹⁶ The label ‘ah’ means apparent horizon.

the limit case, where $t_s = \phi_0$ and tachyon field vanishes, the potential diverges¹⁷.

We leave to subsection III.B (at about Fig. 7) for a discussion on the physical correspondence of (b) (or [a]) in terms of gravitational collapse; Notwithstanding its contribution, the fact is that $V(\phi) \sim \phi^{-2}$ and $\phi \rightarrow 0$ may not be suitable for a realistic (as far as string theory is concerned) appraisal of a tachyon field as $\phi \rightarrow 0$.

- Point (c): For this critical point, the eigenvalues are $\zeta_1 = 0$, and $\zeta_2 = y_0^2 + \frac{\lambda^2}{6}y_0$. The exponential term $\exp(\zeta_2\tau)$ increases as τ gets larger; Hence, the trajectories near this point diverge in the corresponding equilibrium subspace; This means that asymptotically it is *unstable*¹⁸ (source).

Subsequently, the time dependence of the tachyon field can be presented integrating $\dot{\phi} = -\lambda\sqrt{\frac{y_0}{3}}$, as

$$\phi(t) \simeq -\lambda\sqrt{\frac{y_0}{3}}t + \phi_0. \quad (38)$$

In the $\phi > 0$ branch (where $\lambda > 0$), the tachyon field decreases from an initial configuration at $t = 0$ where $\phi_0 > 0$. A possible evolution (i.e., class of solutions) can be as such: The tachyon is moving uphill the potential, with ϕ decreasing; Then, at the singular time $t_s < \lambda\sqrt{3/y_0}$, the tachyon field reaches its nonzero minimum as ϕ_s , while the potential reaches its maximum (but finite) value. The dynamical variable $y = \frac{V}{3H^2}$ approaches y_0 asymptotically at $t = t_s$. With $y_0 > 0$ being constant, the Hubble rate reads $H = -\sqrt{V/3y_0}$ at t_s . Hence,

¹⁷ On the other hand, for the $\phi < 0$ branch as the collapsing system evolves from an initial condition at $t = 0$ where $\phi_0 < 0$, as time proceeds, the tachyon field may decrease to more negative values, in a downhill motion, within the potential, towards [b]. Then, as the collapse reaches $t = t_s$, the potential reaches its minimum as the tachyon field reaches $\phi_s < 0$. Meanwhile, the Hubble rate diverges and (for the largest value in terms of $|\phi_s|$) the dynamical variable $y = \frac{V}{3H^2}$ asymptotically vanishes.

¹⁸ For this fixed point, the eigenvalues values are real, with one being zero and other is positive. The phase portrait for this fixed point is degenerate: The Jacobi matrix \mathcal{A} has a one-dimensional nontrivial null space; Any vector in the null space of \mathcal{A} is an equilibrium point for the system. That is, the system has an equilibrium subspace rather than an equilibrium point. To analyze the phase space portrait, we may define a matrix $M \equiv [v_1, v_2]$, where v_1 and v_2 are the associated eigenvectors of the matrix $\mathcal{A} = [\zeta_1, \zeta_2]$, the diagonal form of Jacobi matrix. Note that v_1 spans the null space of \mathcal{A} . The change of variable $(x(\tau), y(\tau)) \rightarrow (z_1(\tau), z_2(\tau))$, where $(z_1, z_2) = M^{-1}(x, y)$, results in a new set of dynamical equations: $\partial z_1/\partial\tau = 0$, $\partial z_2/\partial\tau = \zeta_2 z_2$, whose solutions are $z_1(\tau) = z_{10} = \text{constant}$, and $z_2(\tau) = z_{20} \exp(\zeta_2\tau)$. Hence, with $\zeta_2 > 0$, the exponential term increases with τ . Thus, all trajectories diverge away from the equilibrium subspace. I.e., (c) is *unstable* (source) [41].

the energy density ρ_ϕ remains finite at this point¹⁹; See subsection III.B for a complementary analysis, which brings additional descriptive insights (and solutions) associated to points (c) and [c] alike. The dynamics of the system in the vicinity of (c) is given by $x \simeq \lambda\sqrt{y_0/3}$ and $y \simeq y_0 + y_2(a_0/a)^{3\zeta_2}$, where $\zeta_2 > 0$. From the instability of this point, while a decreases as the collapse evolves, then $x = \frac{\lambda}{\sqrt{3}}\sqrt{y_0}$ remains constant and y varies.

B. Numerical solutions of classical tachyon collapse

Here we complement the qualitative discussion of the previous subsection with a quantitative discussion, by means of sampling the time-dependent behavior of variables like ϕ , a or the energy density ρ .

Let us get more insight and analyse numerically the classical field equations (15)-(20). We import some information, in particular a selection of initial conditions as suggested from the phase space description. We still assume that the potential has qualitatively an inverse power law form, $V(\phi) = \tilde{V}_0\phi^{-\mathcal{P}}$, $\mathcal{P} = 2$, where $\tilde{V}_0 = 1$ for simplicity. In more detail²⁰:

- As before, we can consider solutions along the two different branches of the discontinuous tachyon potential $V(\phi)$, i.e., take $\phi_0 > 0$ and then $\phi_0 < 0$.
- Considering the phase space analysis and particularly the constraint (23), we must verify that the ratio $\frac{V}{3H^2}$ stays in the interval $[0, 1]$ and that the tachyon derivative $\dot{\phi} \in [-1, 1]$ over time. Consequently, this condition imposes some restrictions on the selection of the initial conditions. Figure 2 shows the classical behaviors of the ratio $\frac{V}{3H^2}$ over time for the two branches. It can be seen that during the collapsing time the classical ratio remains in the suitable interval for different settings, showing that a set of initial conditions, adequate to conduct our analysis, can be established.
- Figures 3 and 4 show several solutions for $\dot{\phi}(t)$ in the classical regime and in the allowed region for the ratio $\frac{V}{3H^2}$.
 - In figure 3, for the branch $\phi < 0$, the dotted lines correspond to numerical solutions

¹⁹ For the $\phi < 0$ branch, i.e., the point [c] (with $\lambda < 0$), the tachyon field increases with time from its initial condition at $t = 0$ where $\phi_0 < 0$. In this case, the tachyon can move uphill potential (approaching the singularity) until $t = t_s$. The Hubble rate and the energy density $\rho_\phi = 3H^2$ also increase.

²⁰ With specific initial conditions, will have the same behavior for a given pair $(\dot{\phi}_0, \phi_0)$ as that for one with the “symmetric” pair $(-\dot{\phi}_0, -\phi_0)$.

with initial condition $\dot{\phi}_0 \in [-1, +0.8]$ evolving towards the stable node (point [b]), corresponding to $\dot{\phi}(t) \rightarrow -1$. The dashed lines correspond to numerical solutions with initial condition $\dot{\phi}_0 \in [+0.9, +1]$, evolving towards the stable node (point [a]), corresponding to $\dot{\phi}(t) \rightarrow +1$. This figure also shows that we have an unstable node (point [c]), where a small disturbance either yields a trajectory towards one or the other stable node. In the same figure we have a second plot representing the phase space with coordinates $(\dot{\phi}(t), \frac{V}{3H^2})$, employing (x, y) as the dynamical variables introduced in (22). This last plot complementary represents the classical tachyon collapse with the two mentioned scenarios associated to two stable nodes (point [a] and [b]) being located at $(-1, 0)$ and $(0, +1)$ to which the different trajectories converge. The arrows in the plot show the time evolution, further illustrating the unstable node in the first quadrant, from which the trajectories are diverging, identifying point [c] defined in the previous section.

– In figure 4 we have the situation for branch $\phi > 0$ with the stable nodes at $(-1, 0)$ and $(0, +1)$. However, the unstable node is in this case located in the second quadrant.

– In summary, if we start the collapse with a tachyon field with negative value (cf. figure 3) with, e.g., $\dot{\phi} \in]-1, +0.8[$, the tachyon field runs downhill in the potential $V \propto \phi^{-2}$ and stable node $\dot{\phi} = -1$; There is also a critical point at (x_0, y_0) where we have two scenarios upon a small disturbance: Numerically, either we will have the tachyon field running uphill in the potential (to stable node $\dot{\phi} = +1$) or the tachyon field runs uphill, then stops ($\dot{\phi} = 0$) and start to run downhill towards stable node $\dot{\phi} = -1$. However, if we start the collapse with a tachyon field with positive value (cf. figure 4), with e.g., $\dot{\phi} \in]-0.8, +1[$, the tachyon field runs downhill in the potential $V \propto \phi^{-2}$ and stable node $\dot{\phi} = +1$: There is a critical point at $(-x_0, y_0)$ where we have two possible scenarios with either the tachyon field running uphill in the potential (to stable node $\dot{\phi} = -1$) or the tachyon field runs uphill then stops ($\dot{\phi} = 0$) and start to run downhill towards stable node $\dot{\phi} = +1$.

- Figure 5 shows the classical behavior (dashed for $\phi < 0$ branch and solid for $\phi > 0$) of the scale factor, tachyon field, energy density, pressure and equation of state over time. In this classical regime

the tachyon matter starts to collapse from its initial configuration at $t_i = 0$, with the radius $a(t) = a_0$ and $\dot{\phi} > 0$ initially. Then, a decreases (approaching zero in a finite proper time), the effective energy density diverges (also in finite time) pointing to the formation of a singularity. The tachyon field increases (for branch $\phi > 0$) or decreases (for $\phi < 0$), with its derivative evolving towards the constant values $+1$ and -1 , respectively. This has been described earlier as the stable nodes (point (a) and [b]).

- In figure 6 it is shown, now for a $\dot{\phi} < 0$ initial configuration, how the tachyon starts to collapse from its initial configuration at $t_i = 0$, with the radius $a(t) = a_0$. There, as a decreases (approaching zero in a finite proper time), the energy density diverges.

- It is worthy to mention that the dashed line in Fig. 5 and the solid line in Fig. 6, in the $\dot{\phi}$ plots, reflect how the points (c) and [c] may be identified. More precisely, in the mentioned dashed line in Fig. 5 and the solid line in Fig. 6, $\dot{\phi}$ slightly increases or decreases from an initial value, respectively; A local extremum is reached (cf. the corresponding $\dot{\phi}$ plot) and then decreases or increases, towards [b] or (a), respectively. It therefore conveys the dynamics associated to the presence of (c) or [c] in the corresponding phase space (cf. Figs. 3 and 4).

- As far as trajectories approaching point [a] ($\dot{\phi} \rightarrow +1$) and point (b) ($\dot{\phi} \rightarrow -1$) are concerned, this means, regarding point [a], we need to consider as initial conditions, e.g., $\phi_0 < 0$ and $\dot{\phi}_0 = +0.9$, whereas for point (b), we need $\phi_0 > 0$ and $\dot{\phi}_0 = -0.9$. Without loss of generality, let us discuss point [a]. In figure 7 we have a scenario where the area radius $R(t)$ decreases (approaching zero in a finite proper time), the energy density diverges (also in finite time). The tachyon field $\phi(t)$ increases, without ever crossing the horizontal line $\phi = 0$ and thus never becoming positive (no branch transition allowed). The $\dot{\phi}$ evolves towards $+1$, i.e., point [a]. From this figure we also learn that the larger is the initial value ϕ_0 , the longer the collapse will take. Another interesting feature is the value of the pressure when we start with a small ϕ_0 (see last plot in figure 7): In this last case, the pressure is significantly larger than with a larger ϕ_0 ; Consequently, if we start with a small value for the tachyon field, the collapse will process faster, the area radius will reduce abruptly and this will be characterized with the smooth rise of the pressure until a breakpoint where the pressure starts to drop.

- In figure 8 we depicted the behavior of the mass function as a function of the area radius for several initial ϕ_0 and for $r = 50$. We consider therein the

case where, as the collapse evolves, the $\dot{\phi}$ behavior is associated to point [a]. It is seen that, in the situation where the initial value of tachyon field is lower, the function $\frac{F}{R}$ is highly divergent (and the pressure is higher).

- Within the numerical cases we considered, two outcomes may be found, depending on the behavior of the mass function $F = R\dot{R}^2$, with the area radius $R = ra(t)$.

- In the left plot of figure 9, we see that the mass function starts to increase from its initial value at $t_i = 0$; However, it remains less than the area radius ($\frac{F}{R} < 1$) until the collapse ends in singularity at a finite proper time. This is possible, when the comoving coordinate r is small (in this case we used $r = 10$). Consequently, in this scenario when Θ stays positive up to the singularity, signifying that no trapped surface will form and non-spacelike geodesics can come out of the singularity. Therefore a naked singularity would form.
- However, if r is larger (in this case we used $r = 50$) the ratio $\frac{F}{R}$ gets larger values than unity as the collapse proceeds (right plot in figure 9), causing Θ to tend to negative values. Then, trapped surfaces will form earlier, covering the singularity by an event horizon.

Additional numerical simulations allow to obtain plots like those in Fig. 9, confirming that both types of trajectories approach either points [a] ($\dot{\phi} = +1$) or [b] ($\dot{\phi} = -1$), describing asymptotically a dust-like behavior for the tachyon matter. In this model, as it was mentioned in previous subsection, covering trapped surfaces form for larger values of r before the collapse reaches its final state. Hence, a black hole forms in such conditions.

IV. LOOP QUANTUM EFFECT ON TACHYON FIELD COLLAPSE

We conveyed in the previous section the tachyon classical behavior for a gravitational collapse setting (which is rather different from the case of a standard scalar field; Cf. [13, 24]). However, what will be the outcome in the presence of quantum effects? We will investigate herein this section how non-perturbative loop modifications (cf. [6]) may provide an answer; We consider solely inverse triad corrections.

Let us then proceed and write the Hamiltonian constraint for the tachyon field (see e.g., in [6, 13, 24, 47]) which is given by

$$\mathcal{H}_\phi(\phi, \pi_\phi) = \mathbf{p}^{3/2} \sqrt{V^2 + \mathbf{p}^{-3} \pi_\phi^2}, \quad (39)$$

where the conjugate momentum for the tachyon field $\phi(t)$ reads

$$\pi_\phi = \frac{\partial L}{\partial \dot{\phi}} = \frac{a^3 V(\phi) \dot{\phi}}{\sqrt{1 - \dot{\phi}^2}}, \quad (40)$$

and where $\mathbf{p}^{3/2} \equiv a^3$ is volume parameter [48]; The corresponding energy density and pressure of the tachyon field will now take the form as

$$\rho_\phi = \mathbf{p}^{-3/2} \mathcal{H}_\phi, \quad p_\phi = -\mathbf{p}^{-3/2} \left(\frac{2}{3} \mathbf{p} \frac{\partial \mathcal{H}_\phi}{\partial \mathbf{p}} \right). \quad (41)$$

In the semiclassical corrections regime²¹ (of the inverse triad type) investigated in this section, the term \mathbf{p}^{-1} associated to the momentum operator π_ϕ is replaced by $d_{j,l}(\mathbf{p})$, which is the eigenvalue of the inverse densitized triad operator [50]. Then, the effective Hamiltonian for the tachyon field is re-written as

$$\mathcal{H}_\phi^{loop} = \mathbf{p}^{3/2} \sqrt{V^2 + |d_{j,l}(\mathbf{p})|^3 \pi_\phi^2}, \quad (42)$$

where $d_{j,l}(\mathbf{p}) \equiv \mathbf{p}_j^{-1} D_l(\mathbf{p}/\mathbf{p}_j)$, and (j, l) are two half-integer free quantization parameters [51], $\mathbf{p}_j \equiv (1/3)\gamma j \ell_{\text{Pl}}^2 = a_i^2 j/3 \equiv a_*^2$ [48]. Here a_* is a critical scale at which the eigenvalue of the inverse scale factor has a power-law dependance on the scale factor; $a_i \equiv \sqrt{\gamma} \ell_{\text{Pl}}$ is the scale above which a classical continuous spacetime can be defined and below which the spacetime is discrete [52]. In addition, $\gamma = 0.13$ is the Barbero-Immirzi parameter and ℓ_{Pl} is the Planck length.

We can consider the approximation $l = 3/4$ [53], and then the relation for $D(\mathbf{p}/\mathbf{p}_j)$ which has been given in [50], leads to the following equation as

$$D(q) = (8/77)^6 q^{3/2} \{ 7 \left[(q+1)^{11/4} - |q-1|^{11/4} \right] - 11q \left[(q+1)^{7/4} - \text{sgn}(q-1) |q-1|^{7/4} \right] \}^4, \quad (43)$$

where $q \equiv \mathbf{p}/\mathbf{p}_j = a^2/a_*^2$. This relation for the classical regime, $a \gg a_*$, implies that $D(q) \rightarrow q$, and for the semiclassical regime, $a_i < a \ll a_*$, it reduces to

$$D(q) = \left(\frac{12}{7} q \right)^4. \quad (44)$$

²¹ There is another scenario regarding loop quantum corrections of this type in the regime $a < a_i$, i.e., smaller than the Planck scale. This scheme leads to a Hamiltonian constraint equation as $H^2 \propto \rho(1 - \rho/\rho_c)$, where $\rho_c = \sqrt{3}/(16\pi\gamma^3 G^2 \hbar)$ is the critical loop quantum density, and \hbar is the Planck constant (see [49] and references therein). The region in which the corresponding effective dynamics can be important is the domain in which the term ρ/ρ_c is significant. Then, considering an initial choice for the energy density of the collapsing initial configuration such that $\rho < \rho_c$, we can ignore the ρ^2 modification.

The correspondingly modified Hamiltonian constraint equation follows from $\mathcal{H}^{loop} = -3\dot{a}^2 a + \mathcal{H}_\phi^{loop}$, as

$$3 \left(\frac{\dot{a}}{a} \right)^2 = \frac{V(\phi)q^{3/2}|D(q)|^{3/2}}{\sqrt{q^3|D(q)|^3 - \dot{\phi}^2}}, \quad (45)$$

in which we used the Hamiltonian equation of motion $\dot{\phi} = \partial\mathcal{H}_\phi^{loop}/\partial\pi_\phi$ and equation (42). Then, equation (41) leads to the equation for the effective energy density and pressure in this loop quantum modification, as

$$\rho_\phi^{loop} = \frac{Vq^{3/2}|D(q)|^{3/2}}{\sqrt{q^3|D(q)|^3 - \dot{\phi}^2}}, \quad (46)$$

and

$$p_\phi^{loop} = -\frac{Vq^{3/2}|D(q)|^{3/2}}{\sqrt{q^3|D(q)|^3 - \dot{\phi}^2}} \left[1 + \frac{\dot{\phi}^2 p_j |D(q)|_{,\mathbf{p}}}{q^2 |D(q)|^4} \right], \quad (47)$$

where “ \mathbf{p} ” denotes differentiation with respect to the argument \mathbf{p} . Consequently, we can also retrieve a modified equation of state (cf. (17)) by means of

$$w_\phi^{loop} = - \left[1 + \frac{\dot{\phi}^2 p_j |D(q)|_{,\mathbf{p}}}{q^2 |D(q)|^4} \right]. \quad (48)$$

If we further take, within the regime $a_i < a \ll a_*$, that $q \ll 1$, or $D(q) \ll 1$, the modified equation of motion for the tachyon field is then given by [54]

$$\ddot{\phi} - 12H\dot{\phi} \left[\frac{7}{2} - A^{-1}q^{-15}\dot{\phi}^2 \right] + [Aq^{15} - \dot{\phi}^2] \frac{V_{,\phi}}{V} = 0, \quad (49)$$

where $A \equiv (12/7)^{12}$. Then, the modified Hamiltonian constraint is [54]

$$\rho_\phi^{loop} = 3H^2 = \frac{V(\phi)}{\sqrt{1 - A^{-1}q^{-15}\dot{\phi}^2}}, \quad (50)$$

and for the modified Raychaudhuri equation, we have

$$-p_\phi^{loop} = 2\dot{H} + 3H^2 = \frac{V(\phi)}{\sqrt{1 - A^{-1}q^{-15}\dot{\phi}^2}} \left[1 + \frac{4\dot{\phi}^2}{Aq^{15}} \right]. \quad (51)$$

Subsequently, an effective equation of state can be suggested for this limit, where

$$w_\phi^{loop} \equiv - \left[1 + \frac{4\dot{\phi}^2}{Aq^{15}} \right]. \quad (52)$$

Using the classical energy density $\rho_\phi = \mathbf{p}^{-3/2}\mathcal{H}_\phi$ in (41) and substituting in equation (3), the classical mass function can be given in terms of the classical Hamiltonian of the system as

$$F = \frac{1}{3}r^3\mathcal{H}_\phi. \quad (53)$$

From \mathcal{H}_ϕ in equation (39) and substituting in equation (53) we get

$$F = \frac{1}{3}r^3\mathbf{p}^{3/2}\sqrt{V^2 + \mathbf{p}^{-3}\pi_\phi^2}. \quad (54)$$

Replacing the classical geometrical density term \mathbf{p}^{-1} by $d_{j,l}(\mathbf{p})$ in equation (54) the modified mass function in the semiclassical regime for a tachyon field collapse is now determined as follows

$$F^{loop} = \frac{1}{3}r^3\mathbf{p}^{3/2}\sqrt{V^2 + |d_{j,l}(\mathbf{p})|^3\pi_\phi^2}. \quad (55)$$

Using equation $\dot{\phi} = \partial\mathcal{H}_\phi^{loop}/\partial\pi_\phi$, we may easily get

$$F^{loop} = \frac{1}{3}r^3a^3\frac{Vq^{3/2}|D(q)|^{3/2}}{\sqrt{q^3|D(q)|^3 - \dot{\phi}^2}}, \quad (56)$$

where, using equation (46), it is rewritten as $F^{loop} = 1/3\rho_\phi^{loop}R^3$, with $R(t,r) = a(t)r$. Moreover, within the regime $a \ll a_*$, the modified mass function (56) takes the form

$$F^{loop} = \frac{1}{3}r^3\frac{a^3V(\phi)}{\sqrt{1 - A^{-1}q^{-15}\dot{\phi}^2}}. \quad (57)$$

The behavior of this effective mass function determines whether trapped surfaces will form during the collapse procedure, within the semiclassical regime.

A. Semiclassical tachyon collapse and phase space analysis

In this subsection we will study the collapsing model using a dynamical system description for the equations (49)-(51). We use a new time variable N (instead of the proper time t in the comoving coordinate system $\{t, r, \theta, \varphi\}$). In more concrete terms, we choose

$$N \equiv -\log q^{3/2}, \quad (58)$$

where $q = (a/a_*)^2$, being defined in the interval $0 < N < \infty$; The limit $N \rightarrow 0$ corresponds to the initial condition of the collapsing system ($a \rightarrow a_*$) and the limit $N \rightarrow \infty$ corresponds to $a \rightarrow 0$. For any time dependent function f , we write

$$\frac{df}{dN} \equiv -\frac{\dot{f}}{3H}, \quad (59)$$

where dot denotes the derivative with respect to t .

We herein make use of a *new* set of convenient dynamical variables (cf. (22)), which are adequate to the equations (49)-(51):

$$\begin{aligned} X &\equiv \frac{\dot{\phi}}{A^{1/2}q^{15/2}}, & Y &\equiv \frac{V}{3H^2}, & Z &\equiv A^{1/2}q^{15/2}, \\ \xi &\equiv -\frac{V_{,\phi}}{V^{3/2}}, & \Gamma &\equiv \frac{VV_{,\phi\phi}}{(V_{,\phi})^2}. \end{aligned} \quad (60)$$

Then, equations (49)-(51) are presented as

$$\frac{dX}{dN} = F_1(X, Y, Z, \xi) = X(4X^2 - 9) - \frac{1}{\sqrt{3}}\xi Z\sqrt{Y}(1 - X^2), \quad (61)$$

$$\frac{dY}{dN} = F_2(X, Y, Z, \xi) = XY \left[4X + \frac{1}{\sqrt{3}}\xi Z\sqrt{Y} \right], \quad (62)$$

$$\frac{dZ}{dN} = F_3(X, Y, Z, \xi) = -5Z, \quad (63)$$

$$\frac{d\xi}{dN} = F_4(X, Y, Z, \xi) = -\frac{1}{\sqrt{3}}\xi^2 XZ\sqrt{Y} \left(\Gamma - \frac{3}{2} \right). \quad (64)$$

The Hamiltonian constraint equation is given as

$$\frac{Y}{\sqrt{1 - X^2}} = 1, \quad (65)$$

and note that from (52), we write

$$w_\phi^{loop} = -(1 + 4X^2). \quad (66)$$

Furthermore, note that with $V > 0$, then $Y > 0$, and $-1 < X < 1$, $Z > 0$.

Equations (61), (62), (63), (64) constitute an autonomous system if the functions F_1 , F_2 , F_3 , and F_4 depend only on X , Y , Z , and ξ , but not on the variable Γ ; They cannot as long as Γ is unknown. Therefore, if we *assume* Γ as a function of ξ , namely [55]

$$\Gamma(\xi) \equiv f(\xi) + \frac{3}{2}, \quad (67)$$

then equation (64) becomes

$$\frac{d\xi}{dN} = -\frac{1}{\sqrt{3}}\sqrt{Y}\xi^2 f(\xi) XZ. \quad (68)$$

Hereafter, we take equations (61)-(63) and equation (68) as our dynamical autonomous system. To analyze it, we will find the critical points (X_c, Y_c, Z_c, ξ_c) , solving the set of equations $F_1 = F_2 = F_3 = F_4 = 0$; The properties of each critical point will be determined by the eigenvalues of the Jacobi matrix \mathcal{B} , similar to (29). This leads to a (4×4) -matrix [35]. We restrict ourselves herein this subsection to inverse square potential, presented as

$$V(\phi) = \beta\phi^{-2}, \quad (69)$$

which brings $\xi = \pm 2/\sqrt{\beta}$ as a constant and likewise²² for Γ . Then, the dynamical system reduces to three differential equations with variables (X, Y, Z) . Finally, there

is, under the constraints, just one physical fixed point for the physical system: (P) as $(0, 1, 0)$.

In order to discuss the stability of P , we have to determine the eigenvalues (and eigenvectors) of the matrix below

$$\mathcal{B} = \left(\begin{array}{ccc} \frac{\partial F_1}{\partial X} & \frac{\partial F_1}{\partial Y} & \frac{\partial F_1}{\partial Z} \\ \frac{\partial F_2}{\partial X} & \frac{\partial F_2}{\partial Y} & \frac{\partial F_2}{\partial Z} \\ \frac{\partial F_3}{\partial X} & \frac{\partial F_3}{\partial Y} & \frac{\partial F_3}{\partial Z} \end{array} \right)_{|(X_c, Y_c, Z_c)}. \quad (70)$$

Using equations (61)-(63) and (70), matrix \mathcal{B} becomes

$$\mathcal{B} = \left(\begin{array}{ccc} -9 & 0 & -\frac{\xi}{\sqrt{3}} \\ 0 & 0 & 0 \\ 0 & 0 & -5 \end{array} \right). \quad (71)$$

All eigenvalues are real but one is zero, the rest being negative; This implies that this is a nonlinear autonomous system with a non-hyperbolic point [41]. The asymptotic properties cannot be simply determined by linearization and we need to resort to other method: the center manifold theorem [41]. For convenience, we transform the critical point $P(X_c = 0, Y_c = 1, Z_c = 0)$ to $\tilde{P}(X_c = 0, \tilde{Y}_c = Y_c - 1 = 0, Z_c = 0)$. The autonomous system (61)-(63) is rewritten as

$$\frac{dX}{dN} = F_1(X, \tilde{Y}, Z) = X(4X^2 - 9) - \frac{1}{\sqrt{3}}\xi Z\sqrt{\tilde{Y} + 1}(1 - X^2), \quad (72)$$

$$\frac{d\tilde{Y}}{dN} = \tilde{F}_2(X, \tilde{Y}, Z) = X(\tilde{Y} + 1) \times \left[4X + \frac{1}{\sqrt{3}}\xi Z\sqrt{\tilde{Y} + 1} \right], \quad (73)$$

$$\frac{dZ}{dN} = F_3(X, \tilde{Y}, Z) = -5Z. \quad (74)$$

The eigenvalues of the matrix \mathcal{B} and their corresponding eigenvectors for both fixed points are now

$$\lambda_1 = -9, \psi_1 = \begin{pmatrix} 1 \\ 0 \\ 0 \end{pmatrix}; \lambda_2 = 0, \psi_2 = \begin{pmatrix} 0 \\ 1 \\ 0 \end{pmatrix}; \lambda_3 = -5, \psi_3 = \begin{pmatrix} -\frac{\xi}{4\sqrt{3}} \\ 0 \\ 1 \end{pmatrix}. \quad (75)$$

Let then \mathcal{M} be the matrix whose columns are the eigenvectors of \mathcal{B} ,

$$\mathcal{M} = \begin{pmatrix} 1 & 0 & -\frac{\xi}{4\sqrt{3}} \\ 0 & 1 & 0 \\ 0 & 0 & 1 \end{pmatrix}, \mathcal{T} = \mathcal{M}^{-1} = \begin{pmatrix} 1 & 0 & \frac{\xi}{4\sqrt{3}} \\ 0 & 1 & 0 \\ 0 & 0 & 1 \end{pmatrix} \quad (76)$$

²² Note that, similar to the classical regime, $\xi > 0$ for the $\phi > 0$ branch and $\xi < 0$ for the $\phi < 0$ branch.

Using the similarity transformation \mathcal{T} , the matrix \mathcal{B} can be rewritten as a block diagonal form:

$$\tilde{\mathcal{B}} = \mathcal{T}\mathcal{B}\mathcal{T}^{-1} = \begin{pmatrix} -9 & 0 & 0 \\ 0 & 0 & 0 \\ 0 & 0 & -5 \end{pmatrix} = \begin{pmatrix} \tilde{\mathcal{B}}_1 & 0 \\ 0 & \tilde{\mathcal{B}}_2 \end{pmatrix}. \quad (77)$$

Changing the variables as bellow, we have

$$\begin{pmatrix} X' \\ Y' \\ Z' \end{pmatrix} = \mathcal{T} \begin{pmatrix} X \\ \tilde{Y} \\ Z \end{pmatrix} = \begin{pmatrix} X + \frac{\xi}{4\sqrt{3}}Z \\ \tilde{Y} \\ Z \end{pmatrix}. \quad (78)$$

The dynamical system (61)-(63) in terms of the new variables (X', Y', Z') becomes,

$$\frac{dX'}{dN} = F'_1(X', Y', Z') = \frac{dX}{dN} + \frac{\xi}{4\sqrt{3}} \frac{dZ}{dN}, \quad (79)$$

$$\frac{dY'}{dN} = \frac{d\tilde{Y}}{dN} = F'_2(X', Y', Z'), \quad (80)$$

$$\frac{dZ'}{dN} = \frac{dZ}{dN} = F'_3(X', Y', Z'), \quad (81)$$

where $F'_1(X', Y', Z')$ and $F'_2(X', Y', Z')$ are given by

$$\begin{aligned} F'_1 \equiv & -\frac{1}{\sqrt{3}}\xi Z'(Y'+1)^{1/2} \left(1 - \left(X' - \frac{\xi}{4\sqrt{3}}Z' \right)^2 \right) \\ & + \left(X' - \frac{\xi}{4\sqrt{3}}Z' \right) \left[4 \left(X' - \frac{\xi}{4\sqrt{3}}Z' \right)^2 - 9 \right] \\ & - \frac{5\xi}{4\sqrt{3}}Z', \end{aligned} \quad (82)$$

and

$$\begin{aligned} F'_2 \equiv & \frac{1}{\sqrt{3}}\xi Z'(Y'+1)^{3/2} \left(X' - \frac{\xi}{4\sqrt{3}}Z' \right) \\ & + 4(Y'+1) \left(X' - \frac{\xi}{4\sqrt{3}}Z' \right)^2. \end{aligned} \quad (83)$$

In particular, (79)-(81) have the point of equilibrium $X'_c = Z'_c = Y'_c = 0$. Let us now suppose that we take initial data with $Z' = 0$. Then Z' is zero for all times and we examine the stability²³ of the equilibrium $X'_c = 0$

and $Y'_c = 0$. The corresponding reduced system can now be written as

$$\frac{dY'}{dN} = 4X'^2(1+Y'). \quad (86)$$

Clearly (for initial data near the origin) $X'(t)$ converges exponentially to zero, say, approximately as $\exp(-9N)$. Since Y' is monotonous with N , then the reduced system $dY'/dN \approx 4Y' \exp(-18N)$ will converge as N gets larger, but in general the limit is not zero. Thus, the critical point P is asymptotically *stable*.

The solution in terms of dynamical variables in the neighborhood of the critical point can be presented by making use of equations (28) and (77). From $X(t) = X_c + \delta X$, $Y(t) = Y_c + \delta Y$, and $Z(t) = Z_c + \delta Z$ (cf. equation (27)), it can be easily obtained that

$$X(t) \simeq X_* \left(\frac{a}{a_*} \right)^{27}, \quad Y(t) \simeq 1, \quad Z(t) \simeq A^{1/2} \left(\frac{a}{a_*} \right)^{15}, \quad (87)$$

where $X_* = \dot{\phi}_*$ is the initial value for $\dot{\phi}(t)$ at the time $t = t_*$. Moreover, in neighborhood of the fixed point where $X \ll 1$, the effective energy density (50) can be approximated as

$$\rho_\phi^{loop} \simeq V(\phi) \left(1 + \frac{1}{2} \frac{\dot{\phi}^2}{Aq^{15}} \right). \quad (88)$$

Solution (87) describes the behavior of the trajectories near the origin in the phase space: $\dot{\phi}$ tends very fast to zero as $\dot{\phi} \propto a^{42}$ (where $a \rightarrow 0$); In this approximation the second term in right hand side of (88) evolves as $\dot{\phi}^2/Aq^{15} \propto a^{54}$ and vanishes faster than $\dot{\phi}$. It thus indicates that in this regime, differently from its classical counterpart, the potential of tachyon field has the main role in determining the behavior of the effective energy density of the system $\rho_\phi^{loop} \simeq V(\phi)$ with $\dot{\phi}^2/Aq^{15} \ll 1$. The Hubble rate becomes $H(\phi) \simeq -\sqrt{\beta/3}|\phi|^{-1}$ for the both $\phi > 0$ and $\phi < 0$ branches. Integrating $H(\phi)$, for the scale factor and the tachyon field, we can further ob-

(79)-(81), is $dY'/dN = \mathcal{O}(|Y'|^4)$. Clearly, this cannot assist in reaching any conclusion about the stability. Therefore, we calculate the coefficient h_2 in the series $h(Y') = h_2 Y'^2 + \mathcal{O}(|Y'|^3)$ and study the stability of the origin. The reduced system then reads

$$dY'/dN = 4h_2^2 Y'^4 + \mathcal{O}(|Y'|^5). \quad (84)$$

To get the value of h_2 , we should solve the equation [41]

$$\mathcal{N}(h(Y')) \equiv (\partial h / \partial Y') f'_2 - f'_1 = 0. \quad (85)$$

But this leads to all coefficients being zero valued in the series $h(Y')$. Considering instead $Z' \equiv g(Y') \neq 0$, this will not reach any result, because all coefficients g_i in the series $g(Y')$ are zero as well. Hence we just focus on an analysis of the stability of this fixed point from a qualitative perspective for the reduced system (86).

²³ A description of the center manifold (cf. [41] for more details), is usually retrieved with the assistance of functions $h(Y')$ and $g(Y')$, where $X' \equiv h(Y')$ and $Z' \equiv g(Y')$. Let us assume the solution for h and g to be approximated arbitrary closely as a Taylor series in Y' . Using this method, we can start with the simplest approximation $h(Y') \approx 0$. Then the reduced system, obtained by substituting $X' \equiv h(Y') \neq 0$ and $Z' \equiv g(Y') \approx 0$ in equations

tain

$$\ln |\phi| \simeq -\sqrt{\frac{3}{\beta}} \int \frac{\dot{\phi}}{a} da. \quad (89)$$

Substituting $\dot{\phi} \simeq a^{42}$ in equation (89), the scale factor of the system can be given as

$$a^{42}(\phi) = 42\sqrt{\frac{\beta}{3}} \ln \left| \frac{\phi_s}{\phi} \right|, \quad (90)$$

where ϕ_s is a constant of integration. For an initial condition such as $\phi(0) = \phi_0$, $a(0) = a_* \approx \left(\sqrt{\frac{\beta}{3}} \ln |\phi_s/\phi_0| \right)^{1/42}$, when the tachyon field approaches the finite value as $\phi \rightarrow \phi_s$, the scale factor vanishes as $a \rightarrow 0$. Thus, the potential of tachyon field decreases from its initial value, and approaches a finite value. Then, it is seen that the effective energy density which is given by $\rho_\phi^{loop} \approx \beta/\phi^2$ does not blow up, becoming instead small and remaining finite. On the other hand, the effective mass function is $F^{loop}/R \approx (\beta/3\phi^2)r^2a^2$ and vanishes as $a \rightarrow 0$; That is, no trapped surfaces form for collapsing shells. The effective pressure p_ϕ^{loop} at the neighborhood of this fixed point, for a small scale factor ($a \ll a_*$), is given by

$$p_\phi^{loop} \simeq -V(\phi) \left(1 + \frac{9}{2} \frac{\phi^2}{Aq^{15}} \right), \quad (91)$$

which is negative in the whole semiclassical collapse. Moreover, the effective pressure (91) evolves such that $p_\phi^{loop} \approx -\rho_\phi^{loop} = -\beta/\phi^2$, remaining finite and negative, giving rise to an outward flux of energy in semiclassical regime (cf. subsection IV.B).

Interestingly, in the classical regime, an asymptotic dust-like behavior ($p_\phi \simeq 0$) found for one class of solutions (trajectories) of the tachyon, suggested the formation of trapped surfaces; A non-negative pressure ensures trapped surface formation in an homogeneous tachyon field collapse. Conversely, in the semiclassical counterpart, no trapped surface seems to form in the presence of negative (modified) pressure for the tachyon field cf. subsection IV.B). Moreover, let us add that an Hamilton-Jacobi formulation (c.f. appendix B) allows a similar final state, pointing also (independently) to an outward flux of energy. Finally, from equation (66), it is further seen that the equation of state for matter, as the collapse proceeds ($X > 0$), is $w_\phi^{loop} < -1$ and with $a \rightarrow 0$, then $w_\phi^{loop} \rightarrow -1$.

B. Numerical solutions of semiclassical tachyon collapse

In this subsection, similarly to III.B, we complement the qualitative discussion of the previous subsection by

means of a numerical discussion of variables like ϕ , a or the energy density ρ . We analyze the field equations (49)-(51) in the semiclassical regime, importing a selection of initial conditions as suggested from the phase space analysis. We still assume that the potential has qualitatively an inverse power law form, $V(\phi) = \beta\phi^{-\mathcal{P}}$, $\mathcal{P} = 2$, where $\beta = 1$ for simplicity. In more detail:

- We must have that the ratio $\frac{V}{3H^2}$ stays in the interval $[0, 1]$ and that the tachyon derivative $\dot{\phi} \in [-1, 1]$ over time. This imposes some restrictions on the selection of the initial conditions. Figure 10 shows the semiclassical behavior of the ratio $\frac{V}{3H^2}$ over time. It can be seen that during the collapsing time, the semiclassical ratios remain in the suitable interval, thus pointing to a set of initial conditions adequate to start with. The numerical simulations confirm that $\frac{V}{3H^2}$ is mainly affected by the tachyon field initial value ϕ_* . Furthermore, for smaller ϕ_* , the ratio $\frac{V}{3H^2} \rightarrow 1$ faster and the tachyon field behaves as $V \simeq 3H^2$. Under the change of sign of the initial condition ϕ_* , the ratio behavior does not change. Then:
- Figure 11 shows the semiclassical behavior of the scale factor, tachyon field, effective energy density, effective pressure and effective equation of state over time. In this regime, the tachyon matter starts to collapse from its initial configuration at $t_* = 0$, with the radius $a(t) = a_*$. Then, as a decreases (approaching zero asymptotically), the effective energy density also decreases until reaching a finite constant value. This decay process is very fast, showing that the modified energy density reduces to a constant finite value early in the collapse. The tachyon field evolves towards a negative or positive constant value, depending on the initial sign of the ϕ_* . We also see that $\dot{\phi}$ rapidly approaches zero. The semiclassical effective pressure also has, in the same time range, a local minimum, clearly distinctive from its classical counterpart in figures 5 and 6. Consequently, we have a scenario where the effective energy density remains finite while the system collapses. This is a generic scenario, within the herein used loop correction, in the sense that we get the same behavior for the effective energy density for a large representative set of initial conditions as studied.
- Figure 12 shows the semiclassical behavior of the mass function over time. This result also sustains the phase space analysis done previously for the semiclassical tachyon collapse. More precisely, the function $\frac{E}{R}$ tends to zero early in the collapse process and depends strongly on the initial value of the tachyon field ϕ_* . For very small values of the initial condition ϕ_* , the mass function can start significantly larger than the area radius. However, it

will decrease abruptly approaching zero as the collapse evolves. The energy density also shows the same behavior for small ϕ_* : It will start larger and then reduces to a small and finite constant value.

From the numerical simulations presented in this subsection, the main result is that the loop quantum corrections (of inverse triad type) to the field equations (49)-(51) indicate a scenario where the modified energy density remains finite during the collapse process. Furthermore, another general feature is the behavior of the effective pressure $p_\phi^{loop}(t)$ as depicted in figure 11, as opposed to the classical effective pressure in figures 5 and 6. Both are negative as we can see in (13) and (51). However, in the semiclassical regime the effective pressure is consistently more intense during the collapse. Consequently, the herein loop quantum corrections induces a negative effective pressure, such that it will prevent the formation of a singularity during the tachyon collapse. Moreover, the decreasing energy density suggests an outward flux of energy (see, e.g., [24]). The main point seems to be that while the classical effective energy density diverges, the semiclassical decreases and remains finite.

V. CONCLUSIONS, DISCUSSION AND OUTLOOK

In this paper we considered the marginally bound case of a Lemaitre-Tolman-Bondi model [4, 13, 37] for a gravitational collapsing system constituted by a tachyon matter field ϕ ; Throughout the main text, the potential for the tachyon field was assumed to be of an inverse square form, $V(\phi) \sim \phi^{-2}$. We investigated the classical and a semiclassical regime, the latter characterized by inverse triad corrections [6], aiming at establishing the corresponding final state. In assembling together these two elements (loop quantum effects [6, 24] and tachyonic dynamics [54]), our aim is to extend from the known literature, employing ingredients motivated by recent developments regarding a (high energy) quantum gravity regime:

- Without any loop quantum effects, the equation of motion for tachyon field in a gravitational collapse can be presented as

$$\ddot{\phi} + 3H\dot{\phi}(1 - \dot{\phi}^2) + (1 - \dot{\phi}^2)\frac{V_{,\phi}}{V} = 0. \quad (92)$$

With $-1 < \dot{\phi} < 1$ and $H < 0$, the $\dot{\phi}$ term in (92) acts like an anti-frictional term at a collapsing phase, within an uphill evolution for the ϕ^{-2} potential for tachyon field (i.e., when $\dot{\phi} < 0$). Moreover, the third term (i.e. the term including $\frac{V_{,\phi}}{V}$) has an anti-frictional effect as well. For a downhill tachyonic potential motion, i.e., $\dot{\phi} > 0$, the $\dot{\phi}$ term

together with the last term (i.e., $\frac{V_{,\phi}}{V}$ term) bring friction effects for the collapsing system.

- For a *standard* scalar field in a semiclassical regime, the field equation can be written as [24]

$$\ddot{\phi} + 3H\dot{\phi} - H\dot{\phi}\frac{d \ln D}{d \ln a} + DV_{,\phi} = 0. \quad (93)$$

In a collapsing phase ($H < 0$), considering now a scalar potential as $V \propto \phi^2$, for a downhill motion with $\phi > 0$ initially (i.e. $\dot{\phi} < 0$), the first $\dot{\phi}$ term acts like anti-friction. On the other hand, for a downhill potential motion (when $\dot{\phi} < 0$), the $H\dot{\phi}\frac{d \ln D}{d \ln a}$ term may be also lead a friction or anti-friction influence.

Determining the outcome of the gravitational collapse of a tachyon field, i.e., whether, e.g., a black hole or naked singularity would form, did not correspond to straightforward assessment (cf. with the case of standard scalar field in [13, 24]). We considered an analytical description by means of a phase space analysis [35, 41], discussing several asymptotic behaviors; These were also subject to a study involving a numerical investigation, which added a clearer description of the possible dynamical evolutions. Within the classical setting (cf. subsection III.A), we found analytically a situation where the tachyon evolved towards a dust-like asymptotic behavior; This would suggest a black hole forming. But the mass function behavior seemed to point instead, apparently, to a naked singularity emerging. We then further analyzed the corresponding behavior of trapped surfaces and apparent horizon formation; Numerically (cf. subsection III.B), we took a broad set of initial conditions and parameters values. The appraisal is that a black hole would likely form. Semiclassically, (namely, in the presence of loop corrections of an inverse triad type [6, 54]), although the phase space analysis (cf. subsection IV.A) was more intricate [41], it pointed, fully supported by a wide numerical investigation (cf. subsection IV.B), that the modified equations for the collapse provided a different picture. In particular, we found a class of solutions which showed that the tachyon effective energy remained finite. In addition, the effective mass function stayed less than unity ²⁴; Thus, there were no trapped surfaces forming. In other words, loop quantum corrections of the inverse triad type seem to induce an outward flux of energy at the final state of the collapse (cf. Figure 13). This outcome is further supported by an Hamilton-Jacobi discussion with a $V \sim \phi^{-P}$ potential (cf. Appendix B).

²⁴ Cf. Figures 9 and 12 for an illustration regarding shells in classical and semiclassical regime. It is seen that, in the semiclassical regime, the loop quantum corrections prevent the shells being trapped (with the mass function values being larger than unity), regarding the corresponding classical setting.

We think it is fair to indicate that tachyon gravitation collapse (or scalar field collapse, generally) is still much an open research subject. We employed a specific setting and although we endorse a set of claims and results, quite a few questions remain. Hopefully, these would constitute the aim of future investigations. Let us therefore add, as final comment, that the scope of our research work did not venture in other directions, namely the items mentioned below, likely to be explored within tachyon field collapse:

- A ϕ^{-2} potential was used for the tachyon, whereas for $\phi \rightarrow 0$, the tachyon should not induce a divergent behavior as far as string theory advises [30–34]. In fact, an exponential-like potential for the tachyon could bring a richer set of possible outcomes [27–30], including a better behaved and possibly a more realistic evolution when dealing with $\phi \rightarrow 0$.
- An enlarged phase space (either in terms of dimension, set of critical points and corresponding eigenvalues, i.e., asymptotic dynamics) results when a barotropic fluid is included to the matter sector, besides the tachyon (see, e.g., [35] regarding the classical scenario). Preliminary results [56] show that in this setting, a wider diversity of outcomes is obtained in the semiclassical regime (inverse triad corrections).
- In the herein semiclassical regime, only modifications based on inverse triad corrections were involved. But there are other corrections imported from loop quantum gravity, e.g., holonomies [49] or an “improved dynamics” setting [57].

VI. ACKNOWLEDGMENTS

The authors would like to thank M. Bojowald, C. Kiefer and G. Mena Marugán for making useful suggestions and comments. The authors also thank J. Velhinho for inviting them to a workshop where part of this work was initiated and to A. B. Henriques for conversations on the issue of loop quantum gravity. YT is supported by the Portuguese Agency Fundação para a Ciência e Tecnologia through the fellowship SFRH/BD/43709/2008. He also would like to thank A. Khaleghi and F. C. Mena for useful discussions and J. Carr for useful comments on the issue of the centre manifold theorem. This research work was also supported by the grant CERN/FP/109351/2009 and CERN/FP/116373/2010.

Appendix A: Semiclassical scaling solutions in tachyon collapse

In equations (49)-(51), only two variables are independent. Hence, we can consider three unknown variables:

a , ϕ and V . Let us therefore assume herein a specific scaling-like behavior choice for the scale factor in the semiclassical regime; Subsequently, we will solve for the effective potential in the semiclassical region. Note that we will consider a classical regime that lasts until a transition towards the semiclassical phase occurs, after which loop quantum effects dominate.

It is useful to introduce the set of variables [54, 58],

$$y = a^{-4}, \quad \dot{\chi} = A^{-1/2} q^{-15} \dot{\phi}, \quad U(\chi(\phi)) = 16V(\phi), \quad (\text{A1})$$

which transforms equations (50) and (51) into

$$3K^2(t) = \frac{U(\chi)}{\sqrt{1 - \dot{\chi}^2}}, \quad (\text{A2})$$

and

$$2\dot{K}(t) = -\frac{U(\chi)\dot{\chi}^2}{\sqrt{1 - \dot{\chi}^2}}, \quad (\text{A3})$$

where $K(t) \equiv \dot{y}/y = -4H$ is the Hubble rate for scale factor now represented by $y(t)$. From the tachyon field equation, with a scale factor as $y(t) \sim (t_s - t)^{-k}$, the tachyon field is retrieved as $\chi(t) = \sqrt{2/(3k)}(t_s - t)$ and the potential of the tachyon field is subsequently found as $U(\chi) = \tilde{U}_0 \chi^{-2}$ with $\tilde{U}_0 = 2k\sqrt{1 - 2/(3k)}$. In this semiclassical description, let us therefore write the scale factor $a(t)$, tachyon field $\phi(t)$, and the potential $V(\phi)$, using equation (A1), as

$$a(t) \sim (t_s - t)^m, \quad \phi(t) = \tilde{\phi}_0 (t_s - t)^r, \quad V(\phi) = \tilde{V}_0 \phi^{-\mathcal{P}}, \quad (\text{A4})$$

where $m = k/4 > 0$, $\tilde{\phi}_0 = (2A/(3ka_*^{30}))^{1/2} r^{-1}$, $r = (15m + 1)$, $\tilde{V}_0 = (3k/32)\tilde{U}_0\tilde{\phi}_0^{\mathcal{P}}$, and now $\mathcal{P} = 2/r > 0$, all being constants. It can be seen that for a positive value of m , the effective potential for the tachyon field is always an inverse function of the effective tachyon field ϕ .

The constant t_s denotes herein the time duration for the collapsing system to reach a vanishing scale factor; $a_* = (t_s - t_*)^m$ is the initial radius for the collapse in the semiclassical regime. Moreover, we assume the time for a transition from the classical regime to the semiclassical at $t = t_*$ (cf. Fig 14).

Let us, for simplicity, also assume this time of transition equal to the time t_0 in the classical equation (9), i.e. $t_0 = t_*$. Let us describe in more detail the several elements employed in this appendix. At the boundary of the classical and semiclassical region there is a matching condition at the time $t = t_*$, for the classical scale factor, as given by Eq. (9), and its semiclassical correspondence, in Eq. (A4), namely,

$$(t_s - t_*)^m = a_* = \sqrt{\frac{j}{3}} a_i, \quad (\text{A5})$$

where $a_i = \sqrt{j}\ell_{\text{Pl}}$, separates the region in which the continuous spacetime exists to that in which the spacetime

would be discrete. The time t_* , corresponding to an area radius $R_* = ra_*$, can be determined by choosing the initial condition ($t = 0, a(0)$) of the classical regime, equation (9). Furthermore, the time at which the collapsing system reaches the scale factor a_i , is denoted by t_i and is given by Eq. (A4), as

$$t_i = t_* + a_i^{1/m} \left[\left(\frac{j}{3} \right)^{1/2m} - 1 \right]. \quad (\text{A6})$$

When the scale factor tends to the quantum limit a_i , at $t \rightarrow t_i$, the time interval $t_s - t_i$ is very small. Then the tachyon field and its first time derivative can be approximated as $\phi(t_i) \approx \tilde{\phi}_0(t_s - t_i)^r$ and $\dot{\phi}(t_i) \approx -\tilde{\phi}_0 r(t_s - t_i)^{r-1}$, respectively, which will be vanishingly small. Also the potential $V(\phi)$ in this limit approximates to $V \sim a_i^{-\mathcal{P}}$, and thus will be very large. Equation (A6) further shows the dependence of t_i on the parameter j and the choice of t_* . It indicates that for larger values of j , the longer is the time during which the collapse proceeds towards the quantum limit a_i . On the other hand, for larger values of j , the initial radius in the semiclassical regime, a_* , is larger, and hence the initial area radius in the semiclassical region, R_* will be larger as well.

Let us now address how loop quantum effects (of the inverse triad type) can influence the tachyon collapse within the scope of scaling solutions. Using the solution (A4) of the semiclassical regime, we can rewrite the equation of the effective energy density as follows,

$$\rho_\phi^{loop}(t) = \tilde{\rho}_0 a(t)^{-\frac{2}{m}}, \quad (\text{A7})$$

where²⁵

$$\tilde{\rho}_0 = \frac{\tilde{V}_0 \tilde{\phi}_0^{-\mathcal{P}}}{\sqrt{1 - A^{-1} a_*^{30} r^2 \tilde{\phi}_0^2}}, \quad (\text{A9})$$

is a constant. It is seen from equation (A7) that, for positive values of m , the modified energy density, which is proportional to the modified potential of the tachyon field, is an inverse function of scale factor, behaving as $a^{-2/m}$. The potential of the tachyon field, therefore, directly determines the behavior of the energy density in the semiclassical regime. Hence, when the scale factor starts to decrease, the effective energy density will increase.

The modified mass function can be obtained from equation (3) and the modified Friedmann equation (50):

$$c = \tilde{\rho}_0 a_*^{n - \frac{2}{m}}. \quad (\text{A8})$$

²⁵ The classical energy density ρ_ϕ , Eq. (4), at the boundary of the semiclassical region, should satisfy a matching condition at $t = t_*$, with its semiclassical counterpart ρ_ϕ^{loop} , Eq. (A7). Then, we get a relation for the classical constant c in terms of semiclassical parameters as follows,

We get $F^{loop} = \dot{a}^2 a r^3 = (1/3) a^3 r^3 \rho_\phi^{loop}$ and using (A7), we write

$$\frac{F^{loop}}{R} = \frac{1}{3} r^2 \tilde{\rho}_0 a^{2 - \frac{2}{m}}. \quad (\text{A10})$$

In equation (A10), if the scale factor evolves to a_i , the mass function will tend to $F^{loop} \sim a_i^{3-2/m}$. The modified mass function in the limit $a \sim a_i$ will be vanishingly small, more specifically when the value of m remains in the interval $m > 1$. Therefore, the mass function will be less than the area radius ($F^{loop} < R$) throughout the collapsing scenario. This indicates that no trapped surface will form and the dynamical evolution of the collapse determines a naked singularity. Moreover, for $m > 1$, the effective energy density will diverge near the singularity: From equation (A4), we retrieve that the following ranges $r > 16$, $0 < p < 1/8$ and $k > 4$ correspond to this situation.

Using the equation of state (52), the effective pressure of the tachyon field in the semiclassical regime is given by $p_\phi^{loop} = -(1 + \frac{2}{3m}) \rho_\phi^{loop}$. It can be seen that the weak energy condition, because of $\rho_\phi^{loop} + p_\phi^{loop} = -\frac{2}{3m} \rho_\phi^{loop} < 0$, is violated in the semiclassical regime. Also for $m > 1$, w_ϕ^{loop} should be larger than $-5/3$, which is comparable with its classical counterpart in which $p = -(1 - n/3)\rho$, with $0 < n < 2$. This case ($m > 1$) is accompanied by negative values of the effective pressure, which implies the existence of an outward energy flux as the collapse advances. Since no trapped surfaces form up to the singularity, this outward energy flux would be observable to the outside observers.

If the mass function at scales $a \gg a_*$ in the classical regime is F , whereas for $a < a_*$ (in the semiclassical regime) is F^{loop} , we then get the following expression for the mass loss, as

$$\frac{\Delta F}{F} \equiv \frac{F - F^{loop}}{F} = \left(1 - \frac{\rho^{loop}}{\rho} \right). \quad (\text{A11})$$

Using expressions (10) and (A10) into equation (A11), we obtain

$$\frac{\Delta F}{F} = \left[1 - \left(\frac{\gamma j}{3} \right)^{\frac{1}{m} - \frac{2}{2}} a^{2n - \frac{2}{m}} \right]. \quad (\text{A12})$$

If $n > \frac{1}{m}$, then $\frac{\Delta F}{F} \rightarrow 1$, implying that the mass function in the semiclassical regime tends to zero and the output is an outward energy flux during the dynamical evolution of collapse scenario; Figure 15 shows this evolution of mass loss. It is seen that the mass loss in the semiclassical regime tends to unity very fast and this feature does not depend on the values of parameter j [24]. In this case, a burst of energy is obtained as a naked singularity forms, which is different from the setting in [24], where the naked singularity is resolved.

In order to better understand this scenario, let us consider the geometry outside a spherically symmetric radi-

ating body, as given by the Vaidya metric [38],

$$ds_{out}^2 = - \left(1 - \frac{2M(u)}{r} \right) du^2 - 2dudr + r^2 d\Omega^2, \quad (\text{A13})$$

where $u = t - r$ and $M(u)$ being the retarded null coordinate and the Vaidya mass, respectively. The matching of exterior and interior geometries follows the Israel-Darmois junction conditions, from which we now take the relation $F^{loop} = 2M(u)$ between mass function in loop quantum regime and the Vaidya mass [24]. Let us assume the energy density of the radiation, as measured locally by an observer with a four-velocity vector ξ^μ . Then, the energy flux as well as the energy density of radiation measured in this frame, are given by [59]

$$\sigma \equiv T_{\mu\nu} \xi^\mu \xi^\nu. \quad (\text{A14})$$

We consider only radially moving observers and define the radial velocity for such an observer as

$$V \equiv \xi^r = \frac{dr}{dt}. \quad (\text{A15})$$

Moreover, from $\xi_\mu \xi^\mu = -1$ and $\xi^\theta = \xi^\phi = 0$,

$$\frac{du}{dt} = \xi^u = \frac{\gamma - V}{\left(1 - \frac{2M(u)}{r} \right)} = \frac{1}{\gamma + V}, \quad (\text{A16})$$

where

$$\gamma = \left(1 + V^2 - \frac{2M(u)}{r} \right)^{-1}. \quad (\text{A17})$$

By calculating the non-vanishing component of Ricci tensor (i.e. $R_{uu} = -\frac{2}{r^2} \frac{dM}{du}$) in equation (A14), we get the following expression for the energy flux σ , as

$$\sigma \equiv -\frac{1}{(\gamma + V)^2} \left(\frac{1}{4\pi r^2} \frac{dM(u)}{du} \right). \quad (\text{A18})$$

The total luminosity for an observer with radial velocity V and for the radius r , is given by [59]

$$L(u) = 4\pi r^2 \sigma. \quad (\text{A19})$$

Substituting equation (A18) into the equation of luminosity (A19), we can establish that

$$L(u) = \frac{1}{(\gamma + V)^2} \frac{dM(u)}{du}. \quad (\text{A20})$$

Then, using (A16) in equation (A20), the luminosity in term of the mass function F^{loop} is as bellow,

$$L(u) = \frac{\dot{F}^{loop}}{2(\gamma + V)}. \quad (\text{A21})$$

For an observer being at rest ($V = 0$) at infinity ($r \rightarrow \infty$), the total luminosity of the radiation can be obtained by taking the limit of (A21), as

$$L_\infty(u) = -\frac{\dot{F}^{loop}}{2}. \quad (\text{A22})$$

As long as $dM/du \leq 0$, the total luminosity of energy flux is positive. In terms of mass function, using the solution for scale factor (A4), together with equation (A10), we can write

$$\dot{F}^{loop} = \frac{mr^3}{3} \tilde{\rho}_0 \left(\frac{2}{m} - 3 \right) (t_s - t)^{3(m-1)}, \quad (\text{A23})$$

where it is seen that, for $m > \frac{2}{3}$, the time derivative of the effective mass function is negative, indicating the positiveness of the luminosity (A22). But for $\frac{2}{3} < m < 1$, trapped surfaces will form during the collapse evolution. In this case, a black hole will form and prevent any outward signaling to the distance observer. Meanwhile, for $m > 1$, there is outward flux of energy as naked singularity formation.

Appendix B: Hamilton-Jacobi formulation for the tachyon collapse

In this appendix, we use an Hamilton-Jacobi formulation to investigate the equations of motion for the tachyon field in the presence of loop quantum modifications²⁶ (inverse triad only). This method allows to specify the Hubble parameter as a function of the tachyon field [60]: If the tachyon field is a monotonically varying function of the proper time, then we can present equation (50) in a Hamilton-Jacobi form, as

$$V^2(\phi) = 9H^4 \left[1 - \frac{1}{16\tilde{\beta}} a^{30} H_\phi^2 \right], \quad (\text{B1})$$

with

$$H_\phi \equiv -4\tilde{\beta} \frac{\dot{\phi}}{a^{30}}, \quad (\text{B2})$$

where $\tilde{\beta} = a_*^{30}/A$ is a positive constant and $A \equiv (12/7)^{12}$. Then, the scale factor can be given by the equation below,

$$a^{30}(\phi) = \bar{a}_0 - 120\tilde{\beta} \int \frac{H}{H_\phi} d\phi, \quad (\text{B3})$$

where \bar{a}_0 is a constant of integration. The time dependence of the scale factor $a(t)$ and tachyon field $\phi(t)$ is given by integrating equation (B2), as

$$t - t_* = 4\tilde{\beta} \int \frac{d\phi}{H_\phi a^{30}}, \quad (\text{B4})$$

where t_* is the initial time at the semiclassical regime. Equation (B2) can also be written as

$$H_\phi = \frac{2H_{,\phi}}{3H^2}. \quad (\text{B5})$$

²⁶ Our aim is to complement our investigation in appendix A, concerning scaling solutions.

Equations (B1)-(B4) thus imply that the dynamics of the semiclassical period can be determined once the Hubble parameter $H(\phi)$ has been specified as a function of the tachyon field.

Let us therefore assume a Hubble parameter of the form (see, e.g., [61])

$$H = H_1 \phi^b, \quad (\text{B6})$$

where H_1 and b are arbitrary negative constants, describing a collapsing model. Then, integrating (B3), the scale factor can be obtained as a function of the tachyon field ϕ ,

$$a^{30}(\phi) = B\phi^{2b+2}, \quad b \neq -1, \quad (\text{B7})$$

where $B = -\frac{90H_1^2\tilde{\beta}}{b(b+1)}$ is a positive constant. In (B3), without loss of any generality, \bar{a}_0 has been assumed as $\bar{a}_0 = B\bar{\phi}_0^{2b+2}$ and $\bar{\phi}_0$ is the initial value of the tachyon field at the boundary of the herein semiclassical regime at the time $t = t_*$. Then, (B1) implies that the potential, as a function of the tachyon field, has the form

$$V(\phi) = \bar{V}_0\phi^{2b}, \quad (\text{B8})$$

with the constant $\bar{V}_0 = 3H_1^2(1 + \frac{5b}{2b+2})^{1/2}$. From (B4), we can further obtain the time dependence of the tachyon field as

$$\phi(t) = C(t_s - t)^{-\frac{1}{b}}, \quad (\text{B9})$$

where $C = \left(\frac{15bH_1}{b+1}\right)^{-\frac{1}{b}}$ is a constant and $t_s = t_* + \left(\frac{b+1}{15bH_1}\right)\bar{\phi}_0^{-b}$ is the time for the collapse to be completed. Moreover, the time dependence of the scale factor can have the form

$$a^{30}(t) = D(t_s - t)^{-2-\frac{2}{b}}, \quad (\text{B10})$$

where $D = BC^{2b+2}$ is a positive constant. The initial radius of the collapsing process at the semiclassical regime, $a(t = t_*) = a_*$, corresponding to the initial time t_* , is obtained by using equations (B16)-(B10), as

$$a_*^{30} = \bar{a}_0 = B\bar{\phi}_0^{2b+2}, \quad (\text{B11})$$

where a_* is defined for the semiclassical region by $a_* = \sqrt{\frac{j}{3}}a_i$. This provides the initial value of the effective tachyon field at the boundary of the semiclassical regime, $\bar{\phi}_0 = \phi(t_*)$ (cf. Fig 14). On the other hand, the time corresponding to the limit of the semiclassical spacetime with radius a_i , can be presented as

$$t_i = t_* + C^b B^{15d} \left[\left(\frac{j}{3} \right)^{\frac{15}{2}d} - 1 \right] a_i^{15d}, \quad (\text{B12})$$

where $d = -\frac{b}{1+b}$ is a constant. Using (50), together with (B1) and (B8), the effective energy density can be written as a function of the scale factor, as

$$\rho_\phi^{loop} = \bar{\rho}_0 a^{-30d}, \quad \bar{\rho}_0 = 3H_1^2 D^d. \quad (\text{B13})$$

It is seen that for positive values of d , or the range $-1 < b < 0$ for b , the effective energy density is an inverse function of the scale factor. So, when the collapsing configuration approaches the singularity as $a \rightarrow 0$, the effective energy density would blow up and diverge. The effective mass function $F^{loop}(R)$ can now be obtained by using (57):

$$\frac{F^{loop}}{R} = \frac{1}{3}\bar{\rho}_0 r^2 a^{2-30d}. \quad (\text{B14})$$

This equation shows that for the values $-\frac{1}{17} < b < 0$ the mass function always satisfies $F^{loop} < R$. In this case, there is no trapped surface as the collapse proceeds towards the final state of the collapse in the form of a naked singularity. Comparing (B10) for the scale factor with equation (A4) in Appendix A (discussing scaling solutions), we find that the allowed range for b , concerning the formation of a naked singularity, corresponds to $m > 1$.

For $b = -1$, the Hubble parameter in (B6) takes instead the form

$$H = H_1 \phi^{-1}. \quad (\text{B15})$$

Then, integrating equation (B3), the scale factor as a function of the tachyon field ϕ can be obtained as

$$a^{30}(\phi) = 180\tilde{\beta}H_1^2 \ln \phi, \quad (\text{B16})$$

where the constant of integration \bar{a}_0 in (B3) for this case is given by $\bar{a}_0 = a_*^{30} = 180\tilde{\beta}H_1^2 \ln \bar{\phi}_0$. Using $\tilde{\beta} = a_*^{30}/A$, we can determine the initial value for the tachyon field as $\ln \bar{\phi}_0 = A/(180H_1^2)$. The potential of the system can be established from equation (B1), as

$$V(\phi) = \frac{3H_1^2}{\phi^2} (1 - 5 \ln \phi)^{\frac{1}{2}}. \quad (\text{B17})$$

In this case, the initial value of the potential is given by $\bar{V}_0 = 3H_1^2(1 - 5 \ln \phi)^{1/2}/\bar{\phi}_0^2$, as $a \rightarrow a_*$. On the other hand, the potential of the system for a small scale factor behaves as an inverse square function of the tachyon field: $V(\phi) \simeq 3H_1^2/\phi^2$. The effective energy density for this limit can be obtained by using the Hubble rate (B16) in equation $\rho_\phi^{loop} = 3H^2 = V(\phi)$, leading to

$$\rho_\phi^{loop} = \frac{3H_1^2}{\phi^2}. \quad (\text{B18})$$

Equation (B18) shows that, as $a \rightarrow 0$, the tachyon field and the effective energy density remain finite. Moreover, the effective mass function at this point is $F^{loop}/R \propto H_1^2 a^2$. This relation for the mass function shows that, at the limit $a \rightarrow 0$, when the collapsing tachyon cloud approaches the singularity, the mass function remains less than unity (i.e. $F^{loop}/R \rightarrow 0$). Hence, no trapped surfaces form during collapse evolves: This leads to an outward flux of energy within the setting of the semiclassical regime.

-
- [1] T. P. Singh, Conference Proceedings, TIFR-TAP preprint (1996), India, [arXiv: gr-qc/9606016].
- [2] R. Penrose (1965) *Phys. Rev. Lett.* **14**, 57; S. W. Hawking, *Proc. Roy. Soc. Lond. A* **300**, 187 (1967); S. W. Hawking, and R. Penrose, *Proc. Roy. Soc. Lond. A* **314**, 529 (1970).
- [3] S. W. Hawking, and G. F. R. Ellis, *The Large Scale Structure of Space-Time*, (Cambridge University Press, 1974).
- [4] P. Joshi, *Gravitational Collapse and Space-Time Singularities*, (Cambridge University Press, 2007).
- [5] C. Kiefer, *Quantum Gravity*, Second edition (Oxford University Press, Oxford, 2007).
- [6] M. Bojowald, *Living Rev. Relativity*, **11**, 4 (2008).
- [7] M. Bouhmadi-López, C. Kiefer, B. Sandhöfer, and P. V. Moniz, *Phys. Rev. D* **79**, 124035 (2009), [arXiv: gr-qc/0905.2421].
- [8] E. Greenwood and D. Stojkovic, *JHEP* **06**, 042 (2008).
- [9] M. Choptuik, *Phys. Rev. Lett.* **70**, 9 (1993).
- [10] D. Christodoulou, *Ann. Math.* **140**, 607 (1994).
- [11] R. Penrose, *Nuovo Cimento*, **1**, 252 (1969).
- [12] T. Hertog, G. Horowitz, and K. Maeda, *Phys. Rev. Lett.* **92**, 131101 (2004).
- [13] R. Goswami, and P. Joshi, [arXiv: gr-qc/0410144] (2004).
- [14] R. Penrose, in *Black holes and relativistic stars*, ed. R. Wald (University of Chicago Press, 1998); P. S. Joshi, *Pramana* **55**, 529 (2000); M. Celerier, and P. Szekeres, *Phys. Rev. D* **65**, 123516 (2002).
- [15] A. H. Ziaie, K. Atazadeh and Y. Tavakoli, *Class. Quant. Grav.* **27**, 075016 (2010), [arXiv: gr-qc/1003.1725].
- [16] A. Ori, and T. Piran, *Phys. Rev. Lett.* **59**, 2137 (1987); A. Ori, and T. Piran, *Phys. Rev. D* **42**, 1068 (1990); B. J. Carr, A. A. Coley, M. Goliath, U. S. Nilsson, and C. Uggla, *Class. Quantum Grav.* **18**, 303 (2001); R. Giambó, F. Giannoni, G. Magli, and P. Piccione, *Class. Quantum Grav.* **20**, 4943 (2003); P. S. Joshi and I. H. Dwivedi, *Commun. Math. Phys.* **146**, 333 (1992); T. Harada, *Phys. Rev. D* **58**, 104015 (1998).
- [17] W. A. Hiscock, L. G. Williams, and D. M. Eardley, *Phys. Rev. D* **26**, 751 (1982); Y. Kuroda, *Prog. Theor. Phys.* **72**, 63 (1984); K. Rajagopal and K. Lake, *Phys. Rev. D* **35**, 1531 (1987); I. H. Dwivedi and P. S. Joshi, *Class. Quantum Grav.* **6**, 1599 (1989); P. S. Joshi and I. H. Dwivedi, *Gen. Relativ. Gravit.* **24**, 129 (1992); J. Lemos, *Phys. Rev. Lett.* **68**, 1447 (1992); K. D. Patil, R. V. Saraykar, and S. H. Ghate, *Pramana, J. Phys.* **52**, 553 (1999); S. G. Ghosh and R. V. Saraykar, *Phys. Rev. D* **62**, 107502 (2000).
- [18] D. M. Eardley and L. Smarr, *Phys. Rev. D* **19**, 2239 (1979); D. Christodoulou, *Commun. Phys. (London)* **93**, 171 (1984); P. S. Joshi and T. P. Singh, *Phys. Rev. D* **51**, 6778 (1995); I. H. Dwivedi, and P. S. Joshi, *Class. Quantum Grav.* **14**, 1223 (1997); R. V. Saraykar, and S. H. Ghate, *ibid.* **16**, 281 (1989).
- [19] P. Szekeres, and V. Iyer, *Phys. Rev. D* **47**, 4362 (1993); S. Barve, T. P. Singh, and L. Witten, *Gen. Relativ. Gravit.* **32**, 697 (2000).
- [20] F. C. Mena, B. C. Nolan, and R. Tavakol *Phys. Rev. D* **70**, 084030 (2004); S. G. Gosh, and N. Dadhich, *Gen. Rel. Gravit.* **35**, 359 (2003); T. Harko, S. K. Cheng, *Phys. Lett. A* **226**, 249 (2000).
- [21] P. Binétruy, C. Charmousis, S. C. Davis, J. F. Dufaux, *Phys. Lett. B* **544**, 183 (2002).
- [22] K. Maeda, T. Torii, M. Narita, *Phys. Rev. Lett.* **81**, 5270 (1998).
- [23] M. Bojowald, J. D. Reyes, R. Tibrewala, *Phys. Rev. D* **80**, 084002 (2009); M. Bojowald, T. Harada, R. Tibrewala, *Phys. Rev. D* **78**, 064057 (2008); M. Bojowald, Private communication.
- [24] R. Goswami, P. Joshi and P. Singh, *Phys. Rev. Lett.* **96**, 031302 (2006).
- [25] C. Armendáriz-Picón and V. Mukhanov, *Phys. Rev. D* **63**, 103510 (2001).
- [26] C. Armendáriz-Picón, T. Damour, and V. Mukhanov *Phys. Lett. B* **458**, 209 (1999).
- [27] A. Sen, *J. High Energy Phys.* **12**, 021 (1998).
- [28] A. A. Sen, *J. high Energy Phys.* **04**, 048 (2002); A. A. Sen, *J. high Energy Phys.* **07**, 065 (2002); **16**, 281 (1989); S. H. Ghate, R. V. Saraykar, and K. D. Patil, *Pramana, J. Phys.* **53**, 253 (1999).
- [29] Mohammad R. Garousi, *Nucl. Phys. B* **584**, 284 (2000); E. A. Bergshoeff, M. de Roo, T.C. de Wit, E. Eyras, S. Panda, *J. High Energy Phys.* **05**, 009 (2000).
- [30] A. Feinstein, *Phys. Rev. D* **66**, 063511 (2002).
- [31] Z-K. Guo, Y-G. Cai, and Y-Z. Zhang, *Phys. Rev. D* **68**, 043508 (2003).
- [32] L. R. W. Ambramo and F. Finelli, *Phys. Lett. B* **575**, 165 (2003).
- [33] E. J. Copeland, M. R. Garousi, M. Sami, and S. Tsujikawa, *Phys. Rev. D* **71**, 043003 (2005).
- [34] I. Quiros, T. Gonzalez, D. Gonzalez, Y. Napoles, R. García-Salcedo, and C. Moreno, *Class. Quant. Grav.* **27**, 215021 (2010).
- [35] Juan M. Aguirregabiria, and Ruth Lazkoz, *Phys. Rev. D* **69**, 123502 (2004).
- [36] V. Gorini, A. Kamenshchik, U. Moschella, and V. Pasquier, *Phys. Rev. D* **69**, 123512 (2004).
- [37] G. Lemaitre, *Ann. Soc. Sci. Bruxelles I A* **53**, 51 (1934); R. C. Tolman, *Proc. Natl. Acad. Sci. U. S. A.* **20**, 169 (1934); H. Bondi, *Mon. Not. R. Astron. Soc.* **107**, 410 (1947).
- [38] P. C. Vaidya, *The External Field of a Radiating Star In General Relativity*, *Curr. Sci.* **12**, 183 (1943); P. C. Vaidya, *The Gravitational Field of a Radiating Star*, *Proc. Indian Acad. Sci. A* **33**, 264 (1951); P. C. Vaidya, *Newtonian Time In General Relativity*, *Nature* **171**, 260 (1953).
- [39] T. P. Singh, *Phys. Rev. D* **58**, 024004 (1998).
- [40] E. Malec, N. Ó. Murchadha, *Phys. Rev. D* **47**, 1454 (1993).
- [41] H. K. Khalil, *Nonlinear Systems*, 2nd edition (Englewood Cliffs. NJ: Prentice Hall, 1996); Jack Carr, *Applications of Center Manifold Theorem* (Springer-Verlag, 1981); J. Guckenheimer, P. Holmes, *Nonlinear Oscillations, Dynamical Systems and Bifurcation of Vector Fields* (Springer-Verlag, 1983).
- [42] Imogen P. C. Heard, and David Wands, *Class. Quant. Grav.* **19**, 5435 (2002).
- [43] E. J. Copeland, D. J. Mulryne, N. J. Nunes, and M. Shaeri, *Phys. Rev. D* **77**, 023510 (2008).
- [44] Roberto Giambó, *Class. Quantum Grav.* **22**, 2295 (2005).
- [45] S. Jhingan, P. S. Joshi, and T. P. Singh, *Class. Quant.*

- Grav. **13**, 3057 (1996), [arXiv:gr-qc/9604046].
- [46] J. R. Oppenheimer, and H. Snyder, Phys. Rev. **56**, 455 (1939).
- [47] T. P. Singh and A. Toporensky, Phys. Rev. D **69**, 104008 (2004); G. Date, and G. M. Hossain, Phys. Rev. Lett. **94**, 011302 (2005).
- [48] G. M. Hossain, Class. Quant. Grav. **22**, 2653 (2005).
- [49] P. Singh, Phys. Rev. D **73**, 063508 (2006); Abhay Ashtekar, Gen. Relativ. Gravit. **41**, 707 (2009).
- [50] G. Date, and G. M. Hossain, Class. Quant. Grav. **21**, 4941 (2004).
- [51] M. Bojowald, Class. Quant. Grav. **19**, 5113 (2002).
- [52] M. Bojowald, P. Singh, and A. Skirzewski, Phys. Rev. D **70**, 083517 (2004); P. Singh, and K. Vandersloot, Phys. Rev. D **72**, 084004 (2005).
- [53] M. Bojowald, Phys. Rev. Lett. **89**, 261301 (2002).
- [54] A. A. Sen, Phys. Rev. D **74**, 043501 (2006).
- [55] Wei Fang, and Hui-Qing Lu, Eur. Phys. J. C **68**, 567 (2010).
- [56] Y. Tavakoli, P. Vargas Moniz, J. Marto, A. H. Ziaie, *Tachyon field collapse - II: Barotropic fluid and loop quantum corrections*, in preparation.
- [57] A. Ashtekar, T. Pawłowski, and P. Singh, Phys. Rev. D **74**, 084003 (2006); A. Ashtekar, and E. Wilson-Ewing, Phys. Rev. D **79**, 083535 (2009); M. Martín-Benito, L. J. Garay, and G. A. Mena Marugán, Phys. Rev. D **78**, 083516 (2008); G. A. Mena Marugán, and M. Martín-Benito, Int. J. Mod. Phys. A **24**, 2820 (2009); M. Martín-Benito, G. A. Mena Marugán, and T. Pawłowski, Phys. Rev. D **78**, 064008 (2008).
- [58] T. Padmanabhan, Phys. Rev. D **66**, 021301 (2002).
- [59] R. W. Lindquist, R. A. Schwartz, and C. W. Misner, Phys. Rev. B **137**, 1364 (1965).
- [60] J. E. Lidsey, Phys. Lett. B **273**, 42 (1991); A. G. Muslimov, Class. Quant. Grav. **7**, 231 (1990).
- [61] J. E. Lidsey, J. Cosmol. Astropart. Phys. **12**, 007 (2004).

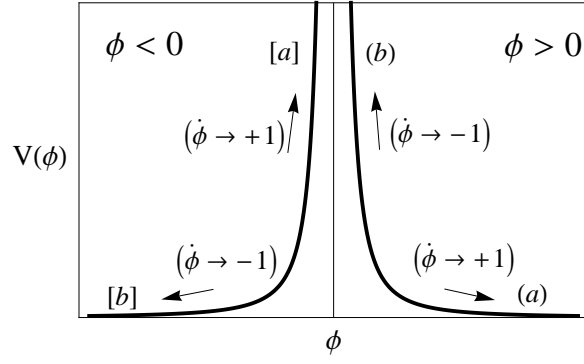


FIG. 1: The potential $V = V_0\phi^{-2}$, denoting the $\phi < 0$ and $\phi > 0$ branches as well as the asymptotic stages.

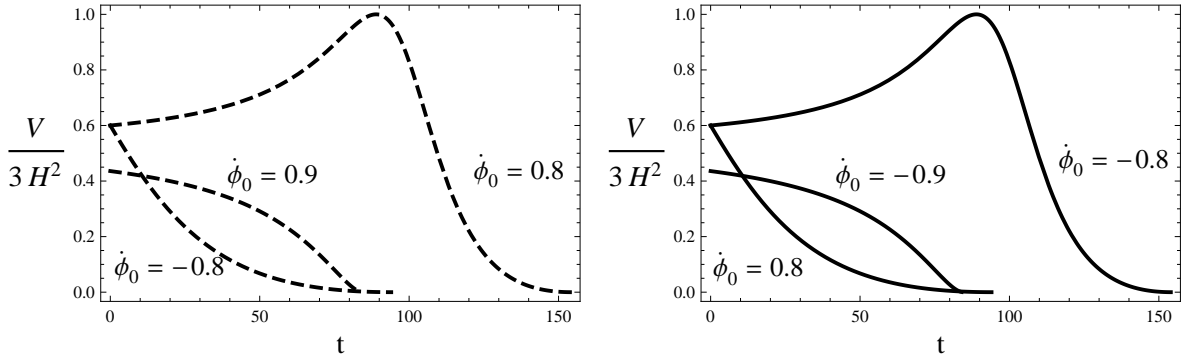


FIG. 2: Behavior of the ratio $\frac{V}{3H^2}$ over time, when the potential of the tachyon field is a power law function; $V(\phi) = \tilde{V}_0\phi^{-\mathcal{P}}$ where $\mathcal{P} = 2$. We considered the initial conditions for this solution as: $t_i = 0$, $a(0) = a_0$. Classical solutions are depicted for $\phi < 0$ branch ($\phi_0 = -100$, dashed) and $\phi > 0$ branch ($\phi_0 = +100$, solid), for some chosen values of $\dot{\phi}_0$.

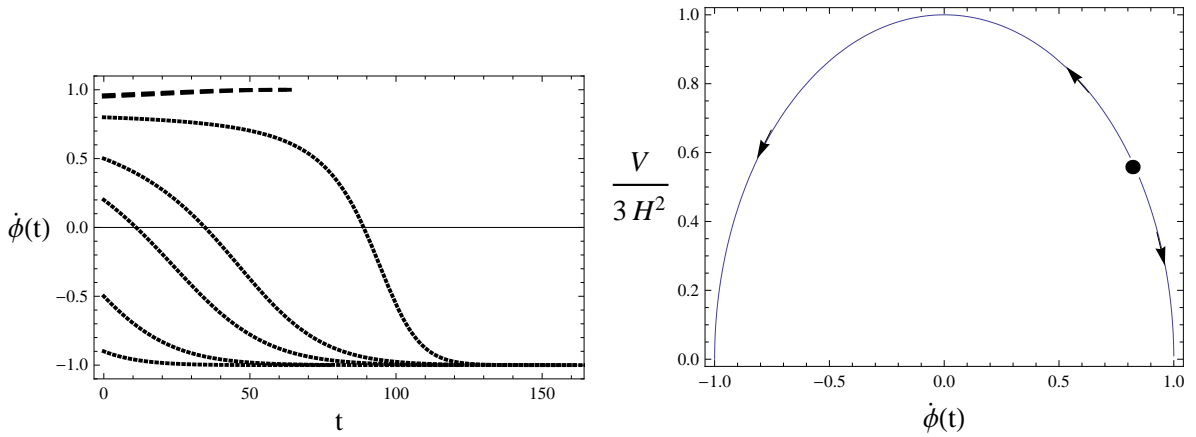


FIG. 3: Behavior of $\dot{\phi}(t)$ (left graphic) for some initial conditions $\dot{\phi}_0 \in]-1, +1[$ and phase space with coordinates $(\dot{\phi}(t), \frac{V}{3H^2})$ for : $t_i = 0$, $a(0) = a_0$, $\phi_0 = -100$.

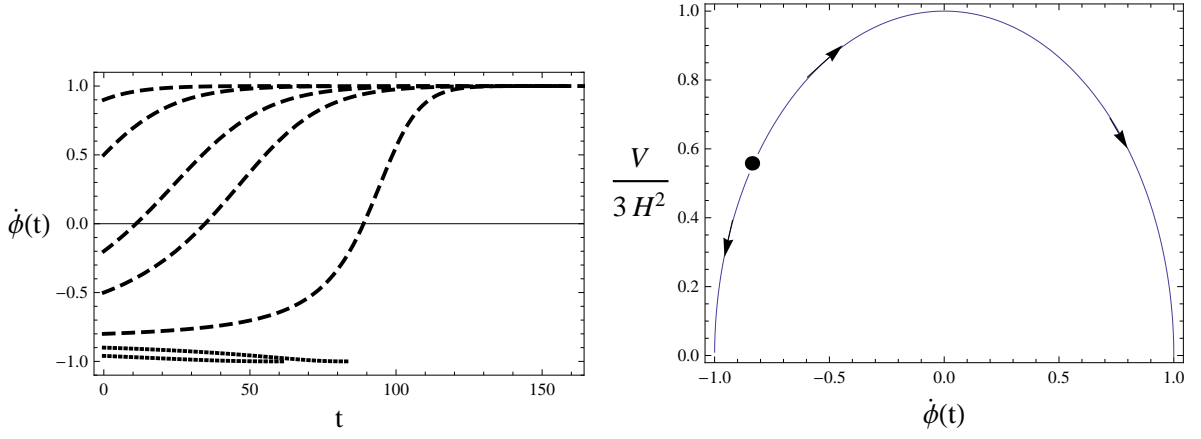


FIG. 4: Behavior of $\dot{\phi}(t)$ (left graphic) for some initial conditions $\dot{\phi}_0 \in]-1, +1[$ and phase space with coordinates $(\dot{\phi}(t), \frac{V}{3H^2})$ for : $t_i = 0, a(0) = a_0, \phi_0 = +100$.

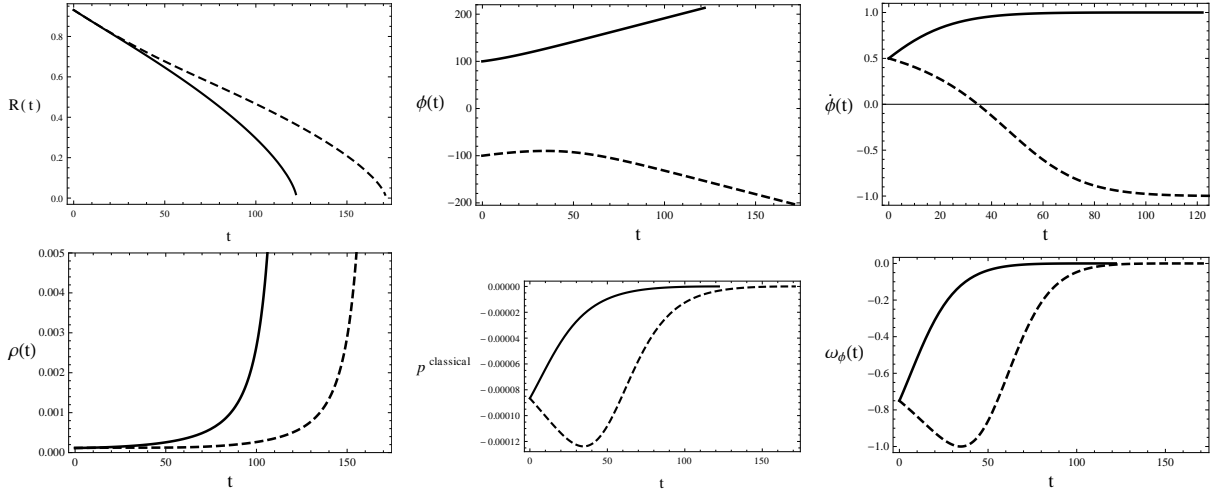


FIG. 5: Behavior of the area radius, tachyon field, energy density, pressure and equation of state over time, when the potential of the tachyon field is a power law function; $V(\phi) = \tilde{V}_0 \phi^{-\mathcal{P}}$ where $\mathcal{P} = 2$. We considered the initial condition for this solution as: $t_i = 0, R(0, r) = ra_0, \dot{\phi}_0 = +0.5$. Classical solutions depicted for $\phi < 0$ branch ($\phi_0 = -100$, dashed) and $\phi > 0$ branch ($\phi_0 = +100$, solid).

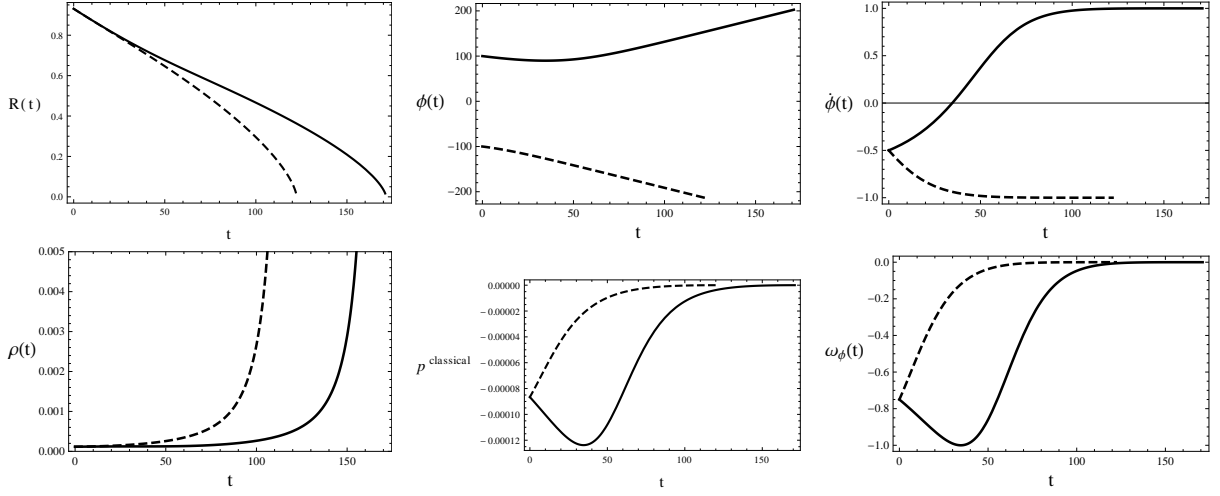


FIG. 6: Behavior of the area radius, tachyon field, energy density, pressure and equation of state over time, when the potential of the tachyon field is a power law function; $V(\phi) = \tilde{V}_0 \phi^{-\mathcal{P}}$ where $\mathcal{P} = 2$. We considered the initial condition for this solution as: $t_i = 0$, $R(0, r) = ra(0) = ra_0$, $\dot{\phi}_0 = -0.5$. Classical solutions depicted for $\phi < 0$ branch ($\phi_0 = -100$, dashed) and $\phi > 0$ branch ($\phi_0 = +100$, solid).

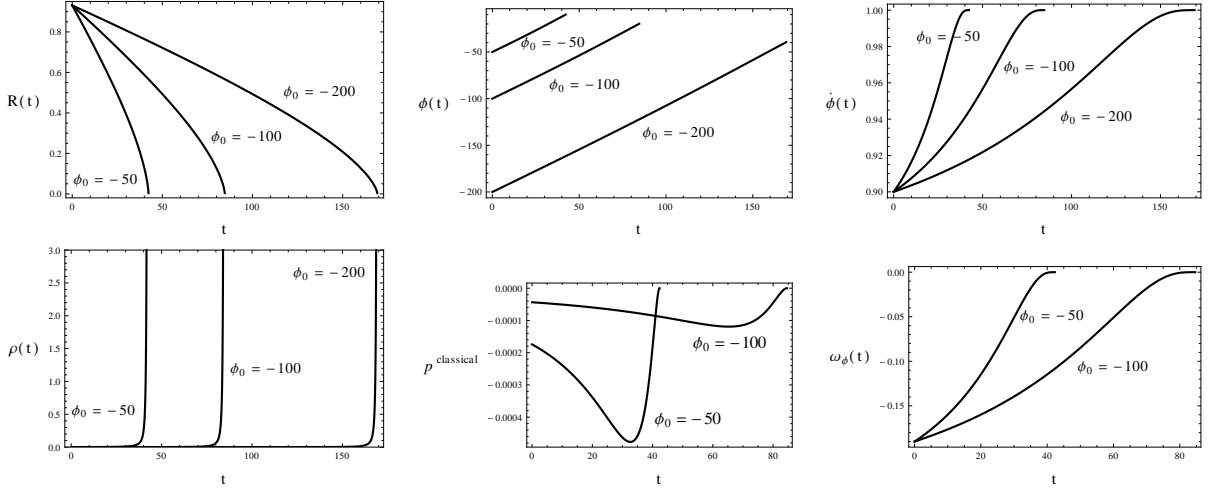


FIG. 7: Behavior of the scale factor, tachyon field, energy density and pressure when the potential of the tachyon field is a power law function; $V(\phi) = \tilde{V}_0 \phi^{-\mathcal{P}}$ where $\mathcal{P} = 2$. We considered the initial condition for this solution as: $t_i = 0$, $R(0, r) = ra(0) = ra_0$, $\dot{\phi}_0 = +0.9$.

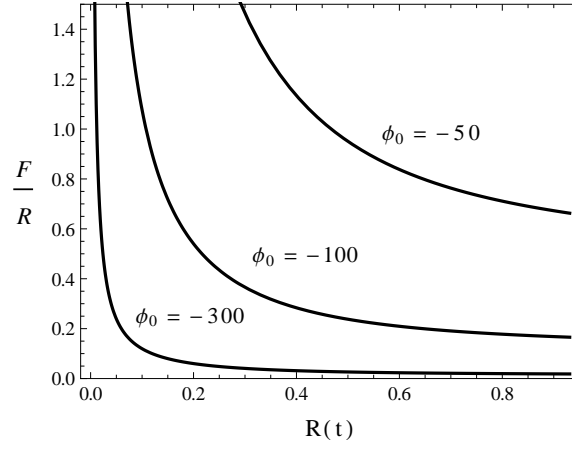


FIG. 8: Classical behavior of the mass function as a function of the area radius, when the potential of the tachyon field is a power law function; $V(\phi) = \tilde{V}_0 \phi^{-\mathcal{P}}$ where $\mathcal{P} = 2$. We considered the initial condition for this solution as: $t_i = 0$, $R(0, r) = ra(0) = ra_0$ and for $\dot{\phi}_0 = +0.9$.

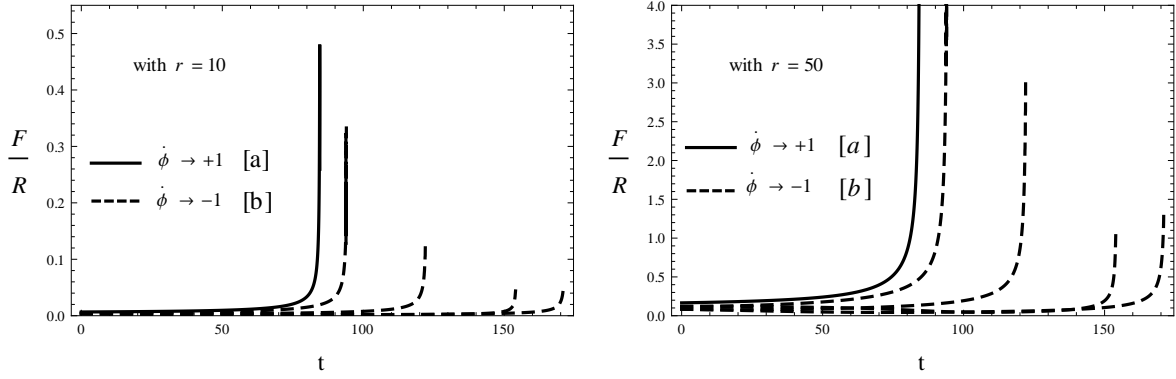


FIG. 9: Classical behavior of the mass function over time, when the potential of the tachyon field is a power law function; $V(\phi) = \tilde{V}_0 \phi^{-\mathcal{P}}$ where $\mathcal{P} = 2$. We considered the initial condition for this solution as: $t_i = 0$, $a(0) = a_0$ and for $\phi < 0$ branch ($\phi_0 = -100$).

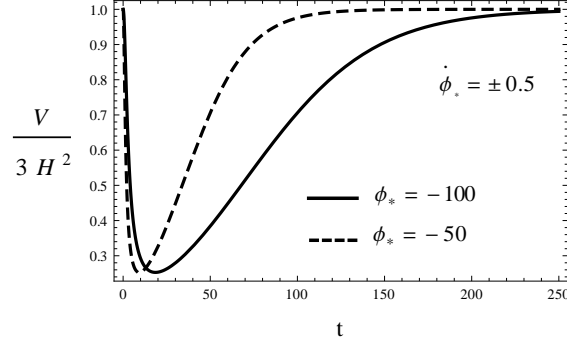


FIG. 10: Semiclassical, with loop corrections, behavior of the ratio $\frac{V}{3H^2}$ over time. The potential of the tachyon field is a power law function; $V(\phi) = \beta \phi^{-\mathcal{P}}$ where $\mathcal{P} = 2$. We considered the initial conditions for this solution as: $t_* = 0$, $a(0) = a_*$.

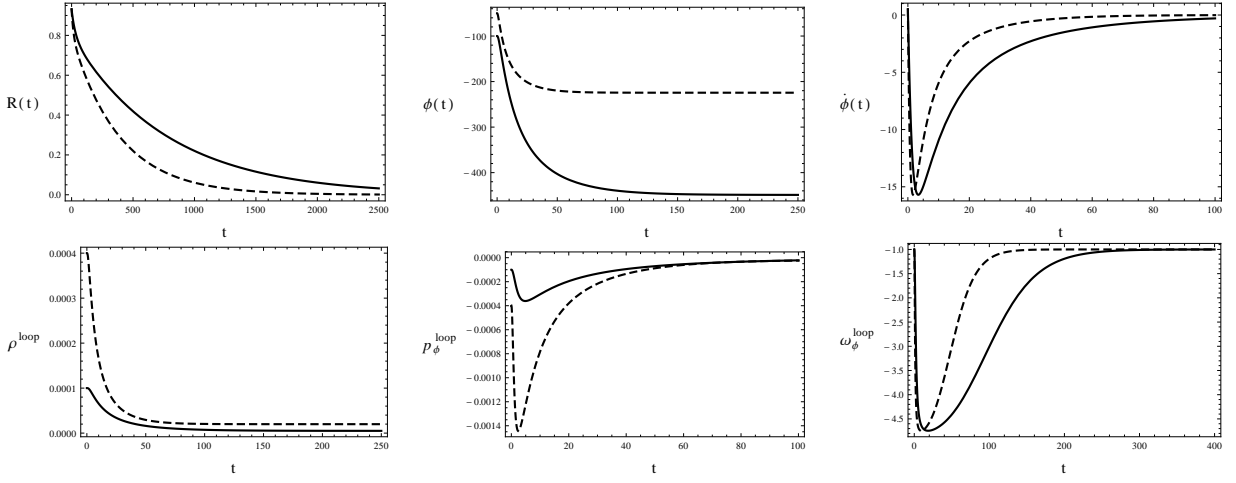


FIG. 11: Semiclassical, with loop corrections, behavior of the area radius, effective energy density, effective pressure and effective equation of state over time, when the potential of the tachyon field is a power law function; $V(\phi) = \beta\phi^{-\mathcal{P}}$ where $\mathcal{P} = 2$. We considered the initial condition: $t_* = 0$, $R(0, r) = ra(0) = ra_*$, $\phi_* = -50$ (dashed), $\phi_* = -100$ (solid), $\phi_* = \pm 0.5$.

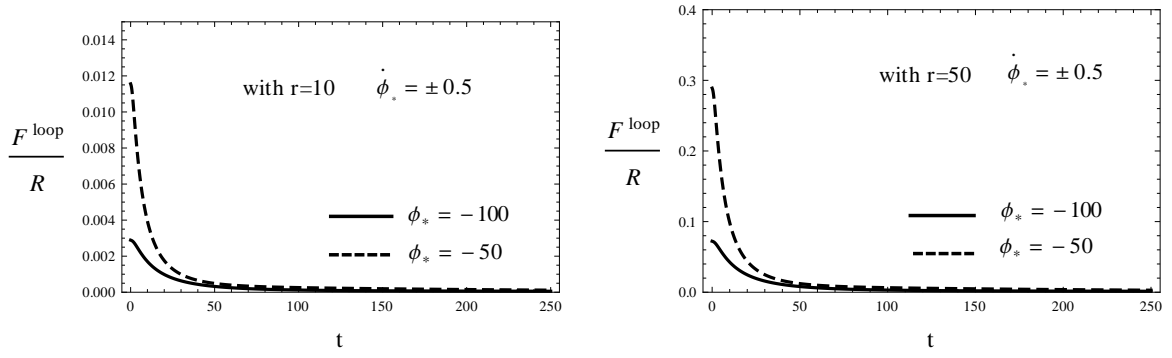


FIG. 12: Semiclassical behavior of the mass function over time, when the potential of the tachyon field is a power law function; $V(\phi) = \beta\phi^{-\mathcal{P}}$ where $\mathcal{P} = 2$. We considered the initial condition for this solution as: $t_* = 0$, $a(0) = a_*$.

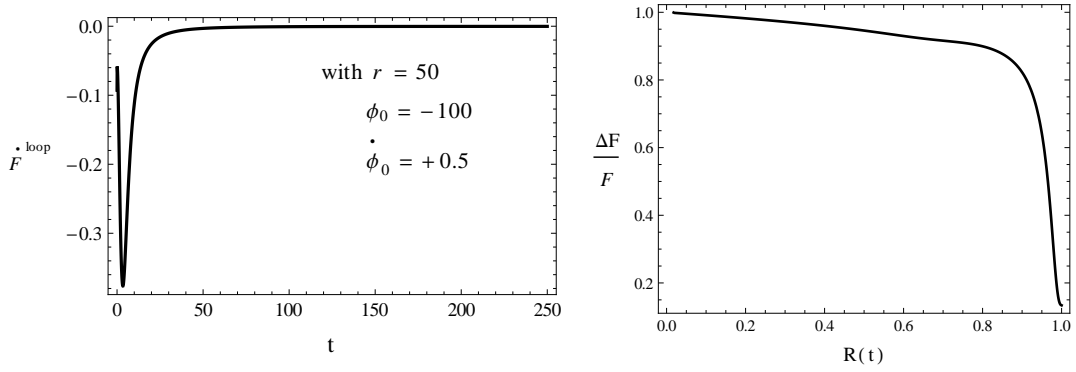


FIG. 13: Behavior of time derivative of mass function (left plot) showing that as the collapse evolves the mass included in the collapsing ball in semiclassical regime keeps decreasing. The right plot shows the behavior of mass loss as a function of area radius of the collapsing shell.

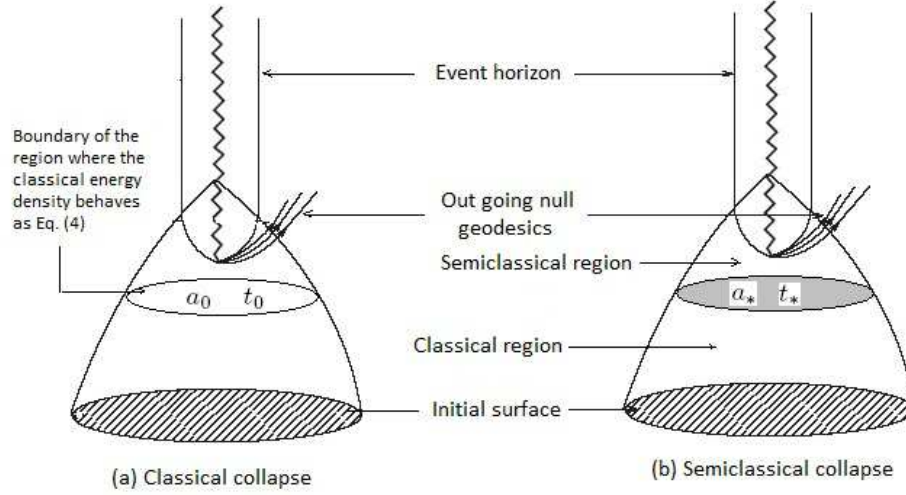


FIG. 14: Two collapsing processes which are started from an initial condition at the same time: (a) A pure classical collapsing system, which starts its evolution from an initial condition on the initial surface; Then at the time t_0 it reaches the radius a_0 . Hereafter the energy density behaves as well as Eq. (4) until the singularity; The final state of the collapse is a naked singularity. (b) Semiclassical collapsing process, in which the tachyon fields starts to collapse from the initial surface, until the boundary of the semiclassical region at time t_* and radius a_* . During this process the dynamical evolution of the collapse is described by the classical equation. Thereafter, the loop quantum modification to the dynamical equations determines the collapsing evolution as long as the continuous spacetime approximations holds.

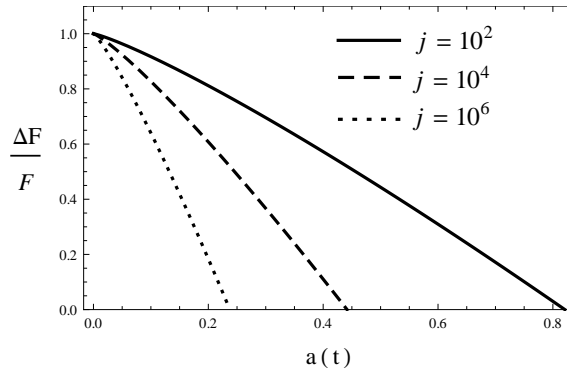


FIG. 15: The behavior of the mass loss with respect to scale factor for different values of j . In this figure, we have respected the inequality $n > 1/m$, where $n = 1.5$ and $m = 1.1$; Both satisfy the ranges determined in the classical section, $0 < n < 2$, and the semiclassical section, $m > 1$, for a naked singularity formation.